UNIVERSITY OF OKLAHOMA

GRADUATE COLLEGE

UTILIZING PALEOMAGNETIC EVIDENCE TO CONSTRAIN THE TIMING OF MAGNETIZATION OF ZEBRA DOLOMITE ACROSS THE GREAT BASIN, NEVADA

A THESIS

SUBMITTED TO THE GRADUATE FACULTY

in partial fulfillment of the requirements for the

Degree of

MASTER OF SCIENCE

By

JARAH BURDETTE

Norman, Oklahoma

2025

UTILIZING PALEOMAGNETIC EVIDENCE TO CONSTRAIN THE TIMING OF MAGNETIZATION OF ZEBRA DOLOMITE ACROSS THE GREAT BASIN, NEVADA

A THESIS APPROVED FOR THE

SCHOOL OF GEOSCIENCES

BY THE COMMITTEE CONSISTING OF

Dr. Shannon Dulin, Chair

Dr. Michael Engel

Dr. Michael Soreghan

ACKNOWLEDGEMENTS

First and foremost, I would like to express my deepest gratitude to my advisor, Dr. Shannon Dulin, whose unwavering support, guidance, and expertise have been invaluable throughout the course of this research. Dr. Dulin not only provided me with critical insights but also encouraged my intellectual growth and creativity. Her mentorship has played a significant role in shaping my academic journey, and I am truly fortunate to have had the opportunity to work under her guidance. I would also like to thank my committee members, Dr. Michael Engel and Dr. Michael Soreghan for their mentorship in providing expertise and insight into my thesis project.

I am also deeply thankful to my family, whose love and support have been a constant source of strength. To my parents and grandparents, thank you for always believing in me and providing a foundation of encouragement, patience, and understanding. Your sacrifices and guidance have made this achievement possible. Your support, both emotionally and practically, has kept me grounded and motivated during the more challenging times of my research. I am forever grateful for everything you all have done to make this journey smoother.

I would also like to extend my sincere appreciation to my colleagues and lab partners. Their collaborative spirit, constructive feedback, and willingness to help with both fieldwork and laboratory tasks have greatly enriched my experience. Thank you specifically to my research colleagues Natalie, Milly, and Joe for sharing your expertise and ideas, which helped to refine and strengthen my research. Our collective efforts and teamwork have made this research a more fulfilling and rewarding experience.

Additionally, I am thankful for the support of my friends, professors, and all those who have inspired me to pursue a career in geology. Whether through their words, actions, or teachings, each of you has contributed to the passion I have for this field. Your encouragement has inspired me to continue exploring the wonders of the Earth, and for that, I am truly grateful.

Lastly, I would like to express my appreciation to all who have influenced and supported me along this journey. Without your encouragement, wisdom, and insight, I would not have reached this point. Thank you all for being a part of my academic and personal growth.

TABLE OF CONTENTS

FIGURES

TABLES

ABSTRACT

Hydrothermal zebra dolomites are a distinct carbonate rock characterized by alternating bands of hydrothermal saddle dolomite (white) layers and darker dolomite layers, typically millimeter thicknesses. The zebra dolomites are often associated with ore mineralization, and are typically described as forming at the same time as the ore laden hydrothermal fluids migrated through the host dolomites. This study uses paleomagnetic techniques to determine if the zebra dolomites hold stable magnetizations that can be used to determine the age of the zebra dolomite formation. These hydrothermal zebra dolomites sampled for this study are hosted in carbonate rocks of Cambrian, Devonian, Mississippian, and Permian age in the eastern part of the Basin and Range Province, Nevada. Of the nine sample locations, six contained characteristic remanent magnetizations (ChRMs) that are interpreted as CRMs held in magnetite based on unblocking temperatures from 360-580ºC. One site had visible reddening, and its ChRM had unblocking temperatures in the range of 540-660 ºC, indicative of maghemite. Twelve CRMs were observed in zebra dolomites across sample localities (some sites held multiple ChRMs). Ten of the twelve CRMs plot on the North American Polar Wander Path (APWP). The CRMs vary in age from Silurian to Jurassic. These multiple ages of magnetization acquisitions reflect the complex tectonic history of Nevada. More sampling of the unaltered non-zebra host rock is needed to determine if these CRMs are localized within the zebra or more widespread. The CRMs are interpreted to date differing fluid pulse conduits over multiple orogenic events throughout the Paleozoic.

INTRODUCTION

Zebra dolomites are a distinct type of carbonate facies characterized by its striking black and white banding, resembling the pattern of a zebra. The banding in the zebra dolomite is comprised of alternating dark and hydrothermal saddle (white) dolomite layers (Figure 1). The dark colored dolomite layers are inferred to be fine grained replacement dolomite, while the hydrothermal saddle dolomite is made up of larger euhedral crystals. The alternating layers are typically on millimeter size scale but can range in size to meter scale in some specific locations within the study area.

Zebra dolomites are found in various geological settings and have garnered attention from geologists due to their ability to capture and preserve key paleoclimate and diagenetic information (Kareem et al., 2019; Kahya et al., 2021). Zebra dolomites can serve as reservoirs for hydrocarbons (Li et al., 2021; McCormick et al., 2023) and are often associated with MVT and Sedex ore deposits in some localities (Diehl et al., 2010). Hydrothermal zebra dolomites in this study are found across the Basin and Range Province of the western United States. Overall, zebra dolomites are quite localized and unique to a few specific locations with their formation thought to be controlled by sedimentary structures within host rocks, tectonics, and/or metasomatism (McCormick et al., 2023). Metasomatism refers to mineralogical and compositional changes due to chemical alteration by a fluid in a pre-existing rock (Lesher & Spera, 2015).

Hydrothermal dolomites hosted within the Basin and Range Province are thought to have formed due to the migration of basinal brines (90-200°C) that coincide with the deposition of Mississippian Valley Type (MVT) and sedimentary exhalative (SEDEX) ore mineralization (Diehl et al., 2010). The age of the zebra dolomites is generally attributed to the age of the ore mineralization, and absolute dating of the zebra dolomites has been difficult to attain. Multiple paleomagnetic studies in this region have addressed the timing of remagnetization of hydrothermal fluid flow events within the Alamo Breccia (Evans et al., 2012), at Delamar Range, Mt. Irish, and Hancock Summit sites of Nevada (Dulin, 2014). Outside of this region, paleomagnetic studies in carbonate formations in the Arbuckles (Elmore et al., 1991) also date remagnetization events. It is known that by using paleomagnetic data it is possible to determine age constraints on these different fluid flow events from the ChRM interpretations. Dulin,

(2014) revealed a late Triassic ChRM in zebra dolomite samples from the Guilmette Formation in southeast Nevada. The late Triassic magnetization was inferred to have been caused by hydrothermal fluid migration during the Triassic Sonoma Orogeny (Dulin, 2014).

Hydrothermal zebra dolomites of this study are found in carbonate rocks of Cambrian, Devonian, Mississippian, and Permian age in central and eastern Nevada. The area of this study lies in the Cambrian, Devonian, Mississippian, and Permian carbonate formations in the southern and eastern parts of the Basin and Range Province, Nevada. Zebra dolomite and host rocks from Apex Quarry, Las Vegas Blvd., Ely, Lee's Canyon, Eureka, Summit, Windfall, Delamar Range, and Wendover, Nevada (Figure 2) were sampled in order to better constrain the timing and formation of zebra dolomites as well as the associated hydrothermal events utilizing paleomagnetic analyses. This study expands the geographic area previously studied and includes zebra dolomites for a wider variety of tectonic and hydrothermal settings. Further constraints on the age of the magnetizations both within the zebra dolomite and the surrounding carbonate rock, will infer the timing of formation and help to better understand the origin of the zebra dolomites.

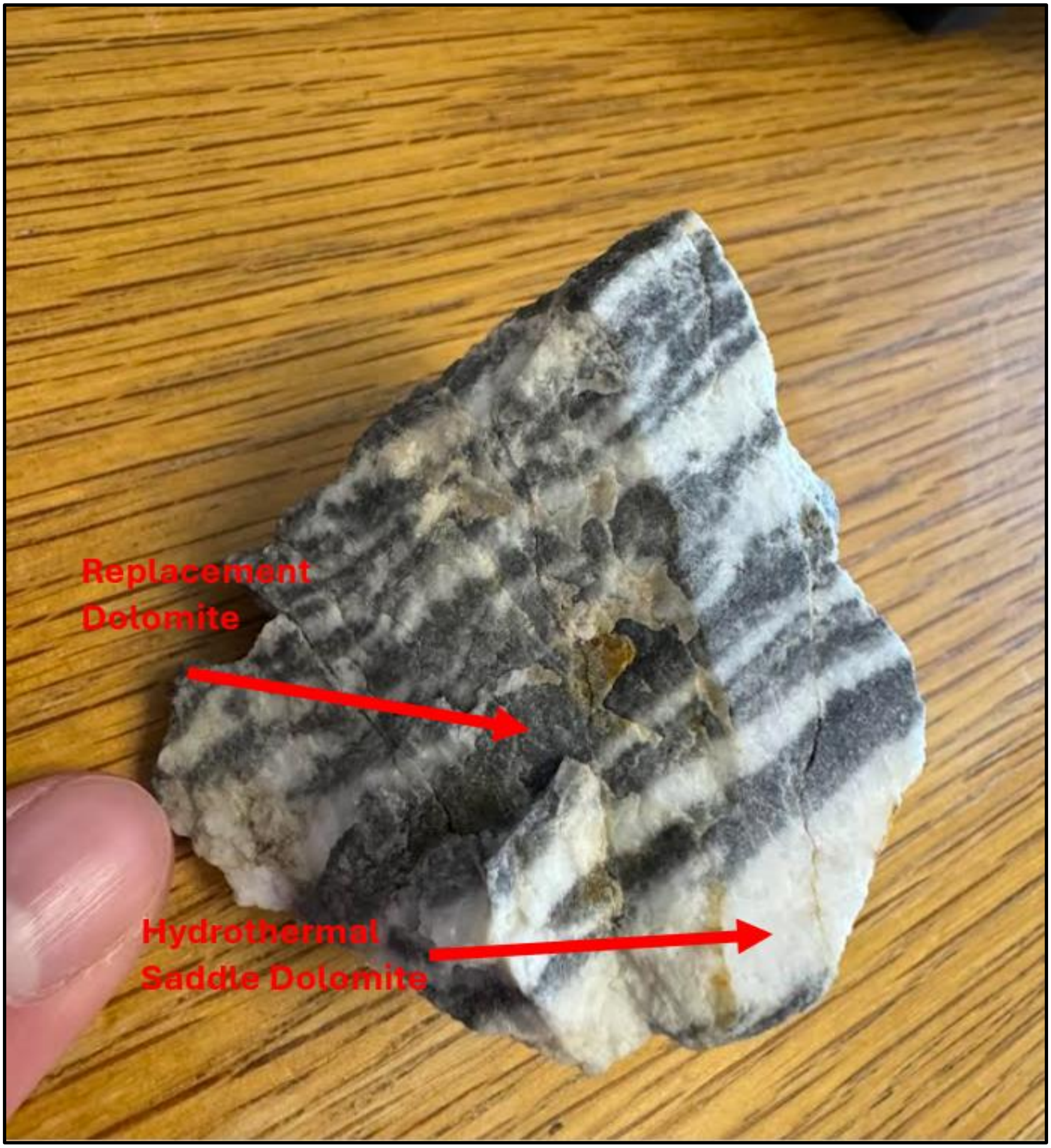

Figure 1: Highlights a hand sample of zebra dolomite from the Delamar Range. Arrows indicate alternating banding of replacement dolomite (black layers) and hydrothermal saddle dolomite (white layers).

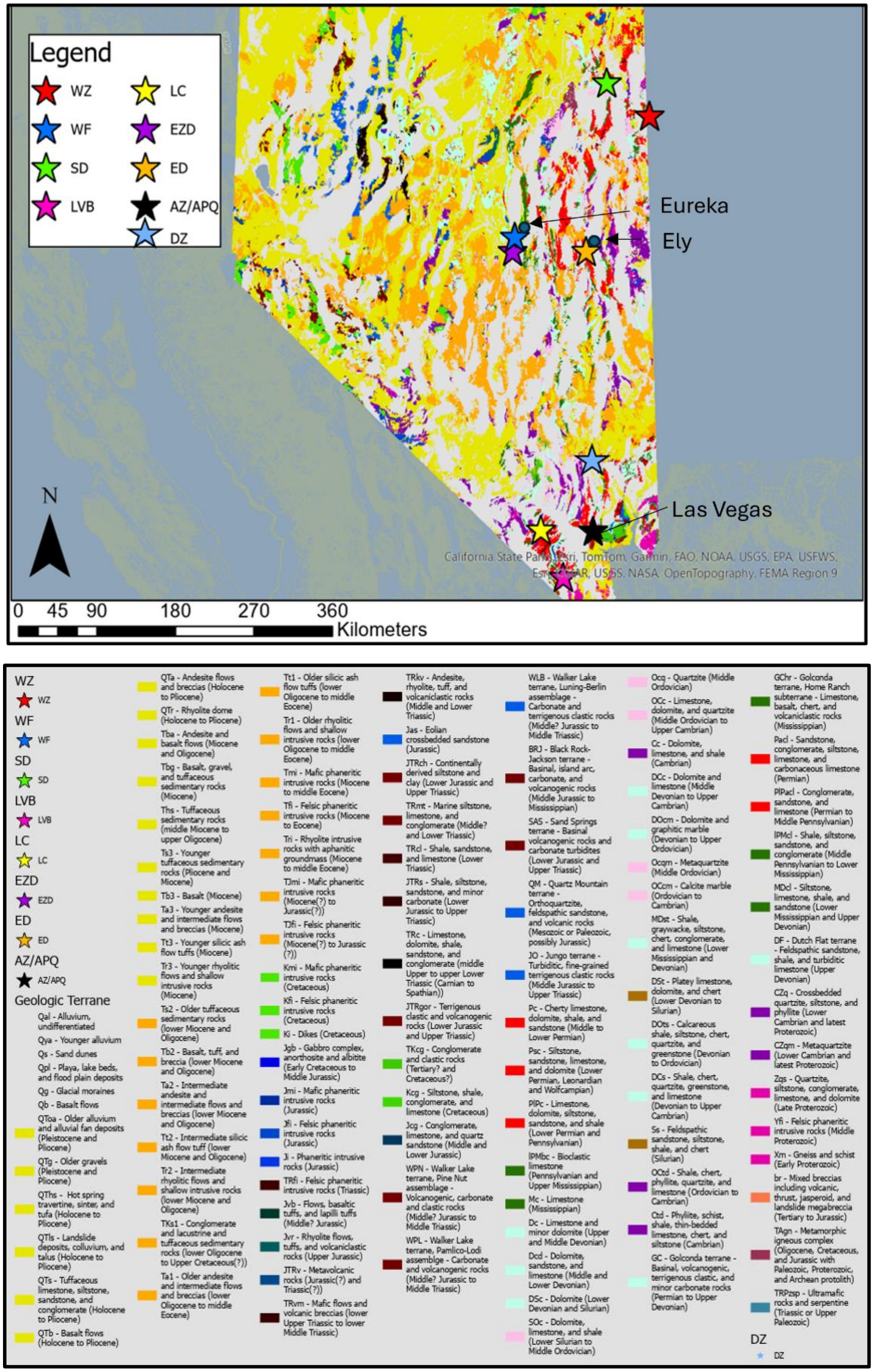

Figure 2: Geologic map and legend of mapped geologic units of Nevada. Stars illustrate zebra dolomite sampling locations of this study. Different colors of geologic units represent units of different geologic age described in the map legend.

Previous Work and Geologic Setting

Zebra dolomites are a distinctive type of carbonate rock characterized by alternating light and dark banding that resembles a zebra's stripes (Figure 1). These banded structures are formed through diagenetic and tectonic processes that can preserve detailed geochemical records of past environmental conditions. Other zebra dolomites are located in western Canada, Africa, Europe, China, and the Middle East (Diehl et al., 2010; Morrow et al., 2014; Kareem et al., 2019; Xu et al., 2022; Kelka et al., 2023; McCormick et al., 2023).

Previous work has attempted to determine the origin of the zebra dolomites. However, the formation of these zebra dolomites is debated due to the small number of occurrences in highly variable geologic and tectonic conditions from across the world which suggests differences in the processes of formation. Previous investigations of zebra dolomite formation have yielded differing interpretations. Initial interpretations inferred that zebra dolomites form from preferential dissolution of sedimentary structures, where dark dolomite replaces the host rock and white hydrothermal dolomite fills cavities (Beales & Hardy, 1980; Morrow et al., 2014). Later studies attributed the formation of zebra dolomites to fractures and fluid flows related to tectonics (Vandeginste et al., 2014; Kareem et al., 2019; Kahya et al., 2021). Other investigations have inferred recrystallization at pressure/temperature conditions near low grade metamorphism (Kelka et al., 2015, 2017; Centrella et al., 2022). Recent basin scale analysis of zebra dolomites in western Canada determined that zebra dolomite formation occurs due to a combination of these factors and possibly relates to multiple fluid flow events (McCormick et al., 2023). Although much work has been done to understand the formation and fabric of zebra dolomites, there has been little evidence to constrain absolute ages of zebra dolomite formation and timing of fluid flow events that facilitated their formation.

The timing of hydrothermal zebra dolomitization (HZD) in eastern Nevada, has largely been inferred based on stratigraphic and spatial relations to ore deposits. Diehl et al. (2010) thoroughly explored zebra dolomites linked to ore mineralization in Nevada, western Utah, and southeastern California. Zebra dolomites were commonly found in proximity to mineral deposits, with Sedimentary Exhalative (SEDEX) and Mississippi Valley Type (MVT) deposits being the most frequent. The study involved sampling zebra dolomites in Cambrian and Mississippian dolostones to investigate their formation process and potential connection to the age of the host rocks and associated ore deposits. Diehl et al., (2010) hypothesized the age of the formation of zebra dolomite as occurring after the deposition of the host rock, as an epigenetic process, though direct dating was not carried out. Diehl et al., (2010) concluded that zebra dolomites formed from hydrothermal activity and were deposited/recrystallized by hot brines (<200°C) that moved along pre-existing faults, which were re-activated during both extensional and compressional tectonic events. Additionally, the formation of ore deposits in Diehl's investigative area of study are hypothesized to correlate with the same hydrothermal fluid events that recrystallized the dolomite with the saddle dolomite creating the zebra fabric (Diehl et al., 2010).

Dulin, (2014) provided a detailed paleomagnetic investigation into three zebra dolomite localities in Nevada at Delmar Range, Mt. Irish, and Hancock Summit in order to determine the timing of zebra dolomite formation by comparison to host rock. Paleomagnetic analysis of hydrothermal zebra dolomite and their associated host rock deposits within the Devonian Guilmette Formation of the Delmar Range uncovered a characteristic remnant magnetization (ChRM) that was removed between 250 – 580 °C. It was interpreted that the ChRM was a chemical remnant magnetization (CRM) residing in magnetite (due to the unblocking temperatures) that was acquired during the Triassic, likely originating from the fluids associated with the Sonoma Orogeny. These migrating hydrothermal fluids may have led to zebra dolomitization (Dulin, 2014).

Gillett and Karlin (2004) carried out a paleomagnetic study on middle Cambrian to upper Pennsylvanian carbonate rocks across the Basin and Range area, including parts of Nevada, Utah, Arizona, and California. These rocks are the host rocks for many of the zebra dolomites in this study. Their research revealed a widespread remagnetization from the late Paleozoic to Triassic periods stored in magnetite throughout the region. The low-inclination magnetization was interpreted as a chemical remanent magnetization (CRM), which likely formed due to the movement of orogenic fluids during the late Paleozoic/early Triassic Sonoma orogeny, the Ancestral Rockies orogeny, or even burial diagenetic processes (Gillett and Karlin, 2004).

Evans et al. (2012) conducted an extensive paleomagnetic analysis of the Alamo Breccia member of the Guilmette Formation at Hancock Summit and Mt. Irish. They identified two magnetic components in and around the breccia at both sites. The first is a syn-tilting intermediate temperature component in pyrrhotite, dating from the Cretaceous to Paleogene period, while the second is a pre-tilting higher-temperature component in magnetite, dating from the

Pennsylvanian to Permian periods (Evans et al., 2012). These magnetizations, similar to those observed by Gillett and Karlin (2004), are thought to be CRMs linked to fluids from external sources. This interpretation is supported by higher $^{87}Sr/^{86}Sr$ ratios found within the Devonian Guilmette Formation.

Zebra dolomite sample sites in eastern Nevada are bounded by the Sonoma and Antlers thrust belts to the west and the Sevier thrust belts to the east. Carbonate deposition on a west-facing slope platform remained constant throughout the Paleozoic in present day Nevada (Diehl et al., 2010). The tectonic history of Nevada is significantly more complex. Pre-Cambrian rifting resulted in a passive margin on the western edge of the North American Plate that lasted into the late Devonian until the North American Plate collided with and subducted beneath the Antlers magmatic arc to the west. This led to a series of north-south trending thrust blocks (Speed and Sleep, 1982).

Following the Antler Orogeny, Nevada returned to a passive margin through the Pennsylvanian. Reactivation of the convergent boundary began in the Late Permian/Triassic with the Sonoma Orogeny (Lawton et al., 2017) and marked an eastward progression of north – south trending fault blocks lasting well into the Jurassic, cutting through the Paleozoic section and providing new migration pathways for basinal hydrothermal fluids to propagate (Speed and Sleep, 1982). During the Triassic through the Jurassic, active subduction led to volcanic arc accretion and associated magmatism further contributing to Nevada's complex geology (Dickinson, 2006). The Cretaceous Sevier Orogeny was another large compressional tectonic event with north-south trending thrust blocks, including episodic extensional pulses (Armstrong, 1968). The present Basin and Range Province formed due to crustal extension (Canada et al., 2019). This Cenozoic Basin and Range extension resulted in high angle normal faulting in the region, forming a series of north-south trending horst and grabens (Stewart, 1980; Canada et al., 2019). The result of Cenozoic tectonics masked much of the earlier tectonic history (Gillett and Karlin, 2004). In addition to the major tectonic events, there are several previously undiscovered or poorly constrained events which are just beginning to be investigated. One such possible episode is the South Laurentian Borderland (SLaB), a trans-tensional tectonic system that occurred in between the Antlers and Sonoma orogenic events (Lawton et al., 2017).

Hydrothermal zebra dolomites of this study are hosted in carbonate rocks of Cambrian, Devonian, Mississippian, and Permian age in the eastern part of the Basin and Range Province, Nevada. In this study, zebra dolomite and host rocks from Apex Quarry (AZ/APQ), Las Vegas Blvd. (LVB), Ely (ED), Lee's Canyon (LC), Eureka (EZD), Summit (SD), Windfall (WF), Delmar (DZ), and Wendover (WZ), Nevada (Figure 2) were sampled in order to better constrain the timing and deposition of zebra dolomites as well as the associated hydrothermal events utilizing paleomagnetic analyses.

At Lee's Canyon (LC) and Windfall (WF) sites, zebra dolomite and host rock samples are from the Cambrian Nopah and Windfall Formations. Zebra dolomite samples from the Eureka (EZD) are held within the Cambrian Hamburg Dolomite. Zebra dolomite localities at Apex (AZ/APQ) and Las Vegas Blvd. (LVB) are held within Mississippian carbonates of the Monte Cristo Formation. Additionally, zebra dolomite samples for Delmar Range (DZ) and Summit (SD) are hosted within carbonates of the Devonian Guilmette Formation. At the Ely (ED) sample site, zebra dolomites are hosted within the Permian Arcturus Formation.

METHODS

Samples (400+) were collected from Cambrian age Hamburg Dolomite, Nopah Formation, and Windfall Formation; Devonian age Guilmette Formation; Mississippian age Monte Cristo Limestone; and Permian age Arcturus Formation. In most instances, samples were collected *in* *situ* using a gasoline-powered Stihl chainsaw modified with a water cooled, 2.5 cm diameter rock coring bit. Prior to removal from the rock, cores were oriented using an inclinometer with a removable azimuthal Brunton compass. Some sites were collected as slabs removed from the sampling location and then cored later. Upon completion of drilling, samples were brought back to the lab, cut into standard 2.5 cm x 2.2 cm plugs and the mass of each plug was measured using a digital SC4010 Ohaus scale.

For petrographic analysis, 20 plugs were sent to Spectrum Petrography where they were prepared as 30 µm, polished thin sections. An additional 16 thin section slides of zebra dolomite from Delmar Range (DZ) were analyzed. Thin sections were analyzed using transmitted and reflected light microscopy to identify mineralogical composition and diagenetic history. Next, the samples were analyzed using a FEI scanning electron microscope (SEM) to verify initial petrographic assessment and resolve mineralogy using energy-dispersive x-ray spectroscopy (EDS).

Stepwise thermal demagnetization was conducted in a magnetically shielded room using 2G Data Acquisition software to control a 2G cryogenic magnetometer with a 581 DC Applied Physics system. Thermal steps measured included: natural remnant magnetization (NRM) up to 600º C in 20ºC steps with demagnetization performed using an ASC Thermal Demagnetizer. Thermal demagnetization data with orthogonal projection diagrams and principal component analysis was used to determine the magnetic component of each sample. This required a minimum of five points when selecting magnetic components, and a combined mean angular deviation (MAD) of ~ 15º or less for a sample to be deemed acceptable. However, most samples have a MAD angle of less than 10º. Means were computed using Fisher (1953) statistics, and the mean was corrected to remove Cenozoic tilting of the beds. Declination and inclination measurements from each component were plotted on an Albers equal-area plot and corrected to current bedding orientations. Once complete, pole positions were calculated (Zijderveld, 1967) and then plotted on the North American Polar Wander Path (Torsvik et al., 2012) to determine approximate timing of remanent magnetizations.

Rock magnetization tests include measuring the Curie temperature using thermomagnetic curve analysis. The Currie point refers to the temperature above which a magnetic mineral will not hold a magnetization; below that temperature the mineral can produce both an induced and a remanent magnetization. This process involves an AGICO KLY5 bridge with a CS-4 furnace, which analyzes how the magnetic properties of a sample change as it is heated from room temperature to 700°C. To prevent oxidation, the tests are conducted under an argon gas atmosphere. The samples, weighing 0.5 grams, are powdered and placed in a quartz tube, where a thermometer measures the temperature changes. The result is a temperature curve that shows the Curie temperature of the magnetic minerals in the sample. These curves are corrected using the Cureval8 software to account for the influence of the quartz tube on the magnetic measurement.

Hysteresis curves and First Order Reversal Curves (FORCs) were obtained using a Lakeshore Cryogenics 8600 Vibrating Sample Magnetometer (VSM). The hysteresis curve was created by magnetizing the sample in one direction and then reversing the field. The inability of magnetic materials to trace back on the same curve is dependent on the magnetic domain of the material. The result measures how the material's magnetization "remembers" the previous field (Ewing, 1930). The FORCs are a set of hysteresis curves that start from a specific saturation field and reveal detailed information about the sample's magnetic domains. For testing, the rock samples were powdered into small chips (0.25 grams), placed in a gel capsule, and attached to a sample rod. The sample was then vibrated between two sensors, which measure the magnetic response as the field strength changes. The resulting data was used to create FORC diagrams that show the type of magnetic domain in the sample.

RESULTS

Paleomagnetic Results:

Southern Nevada

Apex Quarry

The zebra dolomites at the Apex Quarry site were sampled from the Mississippian Monte Cristo Formation. The zebra dolomites at Apex display alternating bands of white saddle dolomite and black bands of precipitated dolomite of similar thicknesses (~2-3mm) over large stratigraphic intervals (Figure 3 A-C).

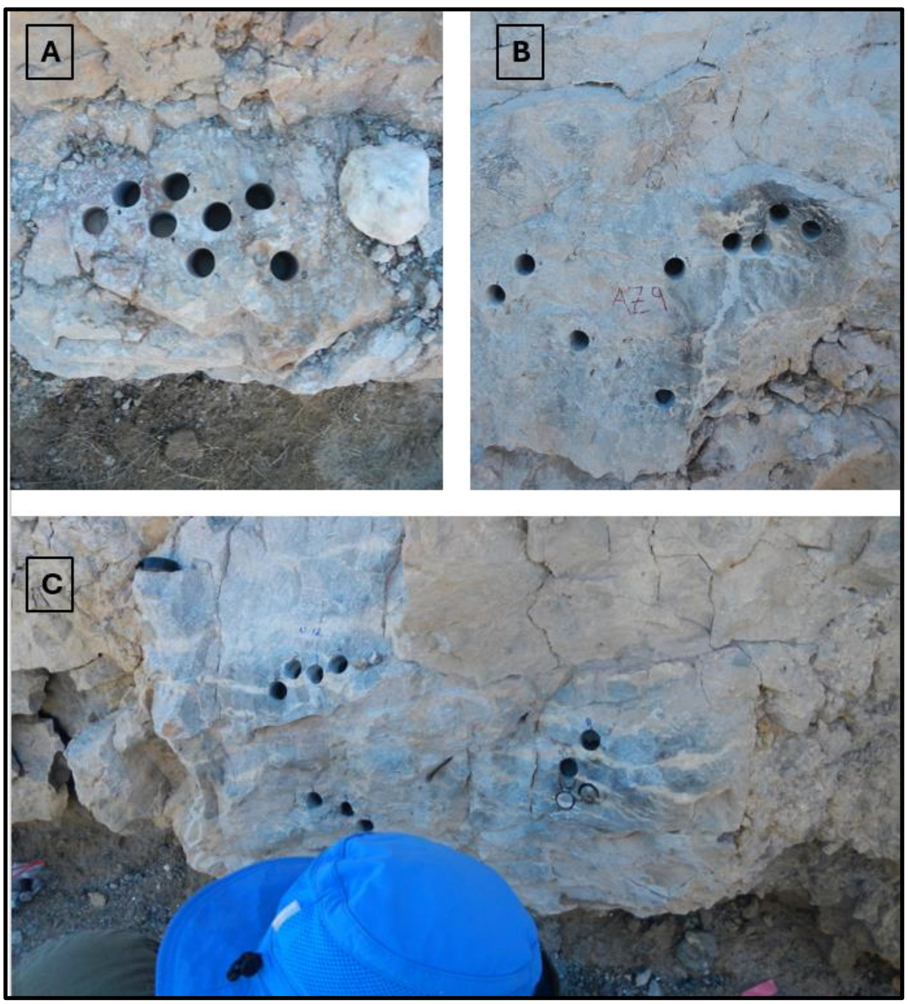

Figure 3: Zebra dolomite sampling sites from Apex location. Localized rhythmic bands of alternating dark replacement dolomite and white saddle dolomite. A) Sample core removal from site AZ5. B) Sample core removal from site AZ7. C) Sample core removal from site AZ12.

Thermal demagnetization at low temperatures (<200°C) removes a northerly and steep down component in many specimens (Figure 4). This is interpreted as the Modern VRM. At higher temperatures, the zebra dolomite at Apex holds two stable ancient magnetizations. The first characteristic remanent magnetization (ChRM) holds northwestern declinations and steep inclinations and is removed between 480-560°C (Table 1). Shown in Figure 4 A-F are orthogonal projection diagrams for zebra dolomite specimens. Figure 4F highlights the equal area plot of specimen directions. The ChRM contains unblocking temperatures below 580°C. This ChRM is observed in all but two of the twelve AZ sample sites.

The second ChRM holds southeastern declinations and shallow inclinations and is removed between 480-560°C (Table 1). Shown in Figure 5 A-D are orthogonal projection diagrams for the zebra dolomites of the second component. Figure 5D illustrates the equal area plot of the second component directions. The ChRM contains unblocking temperatures below 580°C. The second ChRM is only found in AZ9 & AZ11 sample sites.

Mean directions were calculated for both ChRM components of the Apex Quarry zebra dolomites (Table 1). The *in situ* strike and dip of 136/11 was used as the correction for Cenozoic tilting for mean stratigraphic direction of both ChRMs at Apex sample sites. The mean stratigraphic direction of the first ChRM in the zebra dolomite, corrected for Cenozoic extensional tilting, has a declination of 318°, with an inclination of 55.7° ($k = 30.44$, $\alpha95 = 3°$; Table 1). At site AZ 75% of the specimens contain this first ChRM. The first ChRM is held within the majority of the 14 different AZ sample sites except for sites AZ9 & AZ11. Some of the specimens without the first ChRM have low NRM intensities and only contain the VRM.

The mean stratigraphic direction of the second ChRM in the zebra dolomite, corrected for Cenozoic extensional tilting, has a declination of 138.3°, with an inclination of 7.5° ($k = 38.85$, $\alpha95 = 5.7°$; Table 1). Again, *in situ* strike and dip of 136/11 were used as the correction for Cenozoic tilting for mean stratigraphic direction. At site AZ, 82% of the specimens contain the second ChRM. This ChRM is only found in AZ sites 9 & 11.

The stratigraphic mean of the zebra dolomite specimen directions was used to calculate a pole position for each of the ChRMs found at Apex. The calculated virtual geomagnetic pole for the first ChRM is at 57.3°N, 161.1°E ($dp = 3.2°$, $dm = 4.4°$) and the error ellipse intersects the

Middle to Late Jurassic portion of the apparent polar wander path (APWP) for North America (Figure 6) (Torksvik, 2012). The calculated pole for the second ChRM is at 32.2°N, 115.7°E (dp = 2.8°, dm = 5.6°) and lies on the Pennsylvanian portion of the apparent polar wander path (APWP) for North America (Figure 6).

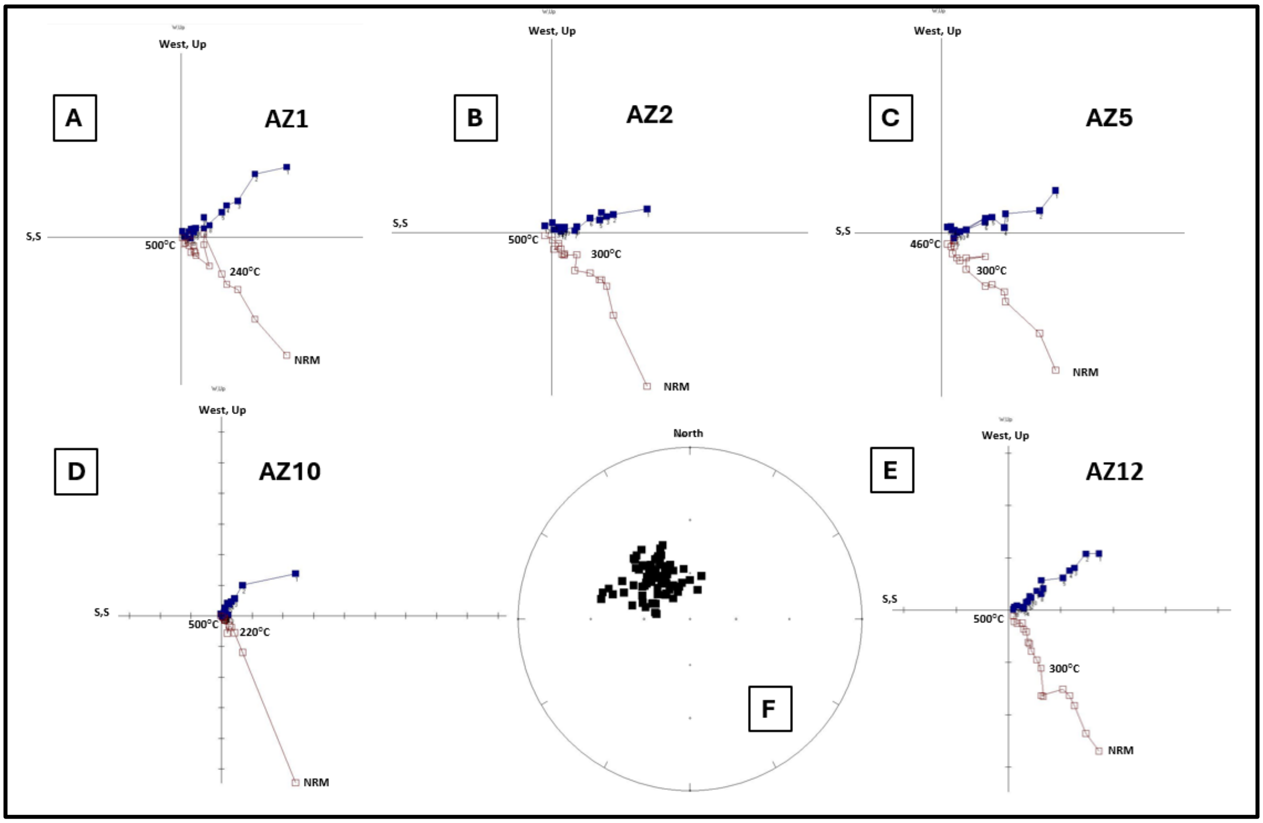

Figure 4: A-E) Orthogonal projection diagrams of representative samples of ChRM I. Closed (open) circles represent horizontal (vertical) component of the magnetic component. F) Equal area plot of specimen directions of all samples that hold the first ChRM at Apex. Closed (open) circles represent positive (negative) inclinations.

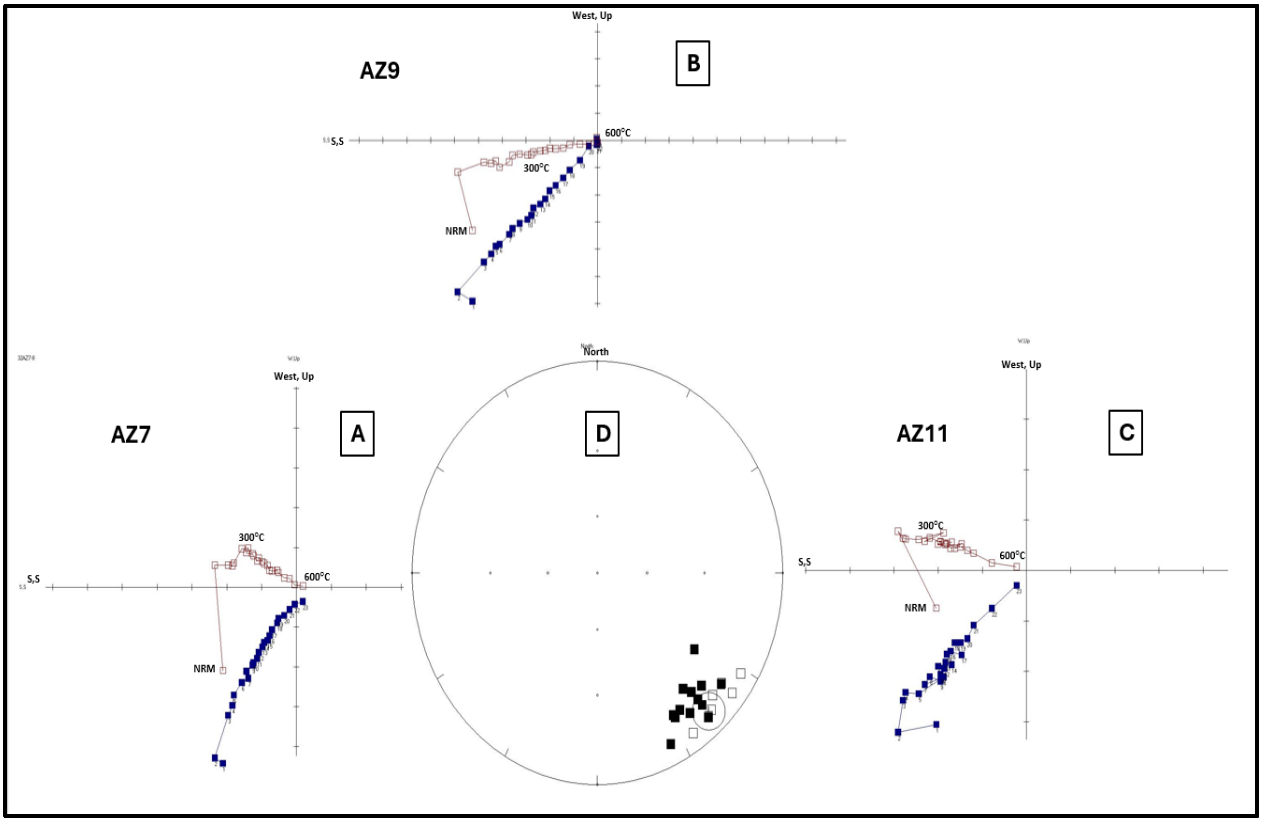

Figure 5 A-D: A-C) Orthogonal projection diagrams of representative samples of ChRM II. Closed (open) circles represent horizontal (vertical) component of the magnetic component. F) Equal area plot of specimen directions of all samples that hold the second ChRM at Apex. Closed (open) circles represent positive (negative) inclinations.

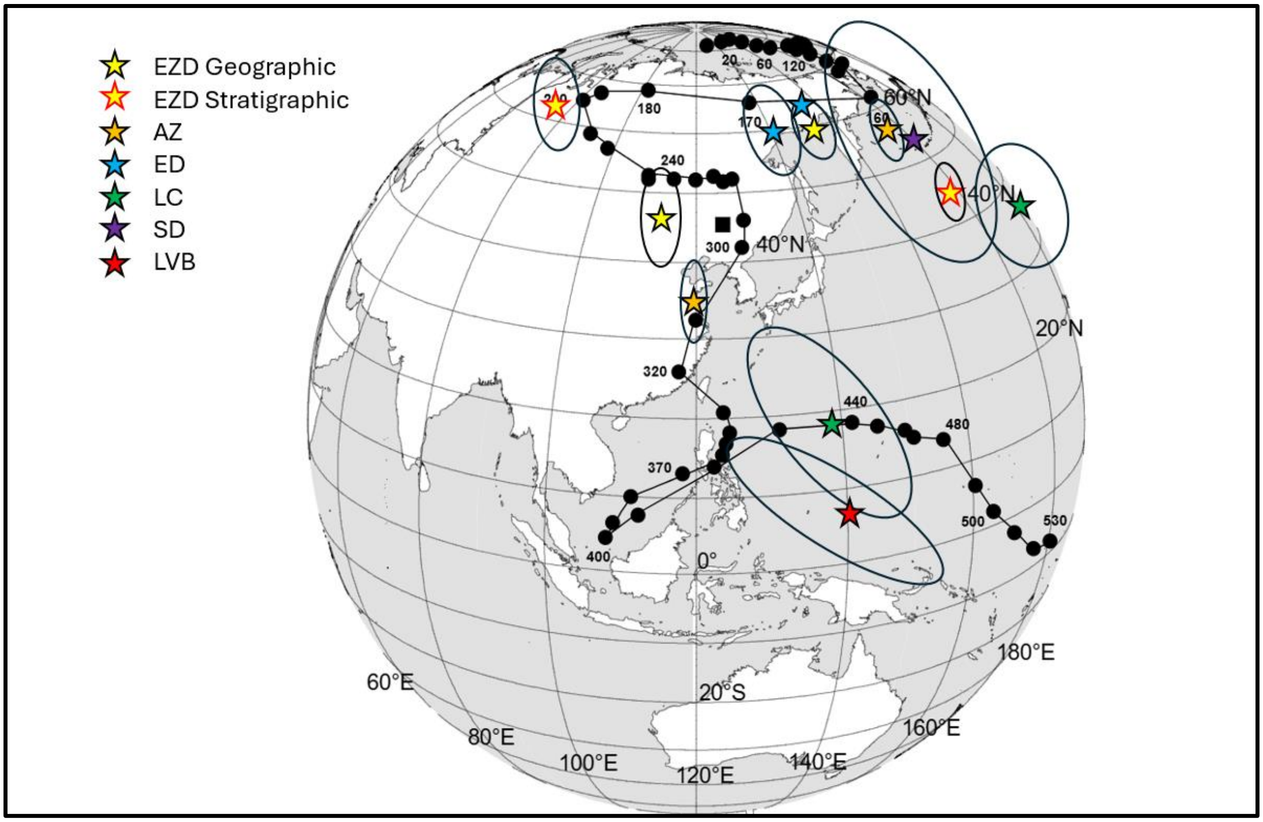

Figure 6: Apparent polar wander path for North America (Torsvik et al., 2012). The different colored stars represent the ChRMs held in zebra dolomites from sampling sites. The two yellow stars with black outlines represent the geographic VGP position of EZD ChRMs. All other stars represent the stratigraphic VGP position from sampling localities in the study. The circles around the stars highlight the associated error ellipse for the VGP at different locations

Lee's Canyon

The zebra dolomites collected from the Lee's Canyon site were sampled from the Cambrian Nopah Formation. The zebra dolomites at Lee's Canyon display alternating bands of white saddle dolomite with light grey to dark bands of precipitated dolomite (Figure 7 A-E). The hydrothermal saddle (white) dolomite bands here are thinner than the samples at Apex (<1mm).

Figure 7: A-E) Zebra dolomite sampling sites from Lee's Canyon location. Localized rhythmic bands of alternating dark replacement dolomite and white saddle dolomite. Sample core removal from LC1-5 sites. C - E show the variation within the zebra dolomite between sites.

Thermal demagnetization at low temperatures (<200°C) removes a northerly and steep down component in many specimens (Figure 8). This is interpreted as the Modern viscous remanent magnetization (VRM). At higher temperatures, the zebra dolomite at Lee's Canyon holds two stable ancient magnetizations. The first characteristic remanent magnetization (ChRM) holds western-northwestern declinations and steep inclinations and is removed between 360-500°C (Table 1). Shown in Figure 8 A-C are orthogonal projection diagrams for zebra dolomite specimens at Lee's Canyon. Figure 8D highlights the equal area plot of specimen directions. The ChRM contains unblocking temperatures between 360-580°C. This ChRM is found in 4 out of 5 sample sites for the Lee's Canyon zebra dolomites (Table 1).

The second ChRM holds eastern declinations and moderate inclinations and is removed between 460-560°C (Table 1). Shown in Figure 9 A-B are orthogonal projection diagrams for the zebra dolomites of the second component. Figure 9C illustrates the equal area plot of the second component directions. The ChRM also contains unblocking temperatures below 580°C. This ChRM was only found at the LC5 sample site.

Mean directions were calculated for both ChRM components of the Lee's Canyon zebra dolomites (Table 1). The *in situ* strike and dip of 110/13 was used as the correction for Cenozoic tilting for mean stratigraphic direction of both ChRMs at Lee's Canyon sample sites. The mean stratigraphic direction of the first ChRM in the zebra dolomite, corrected for Cenozoic extensional tilting, has a declination of 286.9°, with an inclination of 71.3° ($k = 35.71$, $\alpha95 = 4.8°$; Table 1). At sites LC1-LC4, 81% of the specimens contain this first ChRM. The first ChRM is held within the majority of the 5 different LC sample sites. However, it is not present at site LC5. Some of the specimens without the first ChRM have low NRM intensities and only contain the VRM.

The mean stratigraphic direction of the second ChRM in the zebra dolomite, corrected for Cenozoic extensional tilting, has a declination of 84.2°, with an inclination of 40.3° ($k = 35.26$, $\alpha95 = 11.4°$; Table 1). Again, *in situ* strike and dip of 110/13 was used as the correction for Cenozoic tilting for mean stratigraphic direction. At site LC5, 86% of the specimens contain the second ChRM. This ChRM is only found at the LC5 site.

The stratigraphic mean of the zebra dolomite specimen directions was used to calculate a pole position for each of the two ChRMs found at Lee's Canyon. The calculated pole for the first ChRM is at 38.5°N, 201.1°E ($dp = 7.3°$, $dm = 8.4°$) and falls off of the apparent polar wander path (APWP) for North America (Figure 6). The calculated pole for the second ChRM is at 17.8°N, 138.5°E (dp = 8.3°, dm = 13.8°) and plots on the Silurian portion of the apparent polar wander path (APWP) for North America (Figure 6).

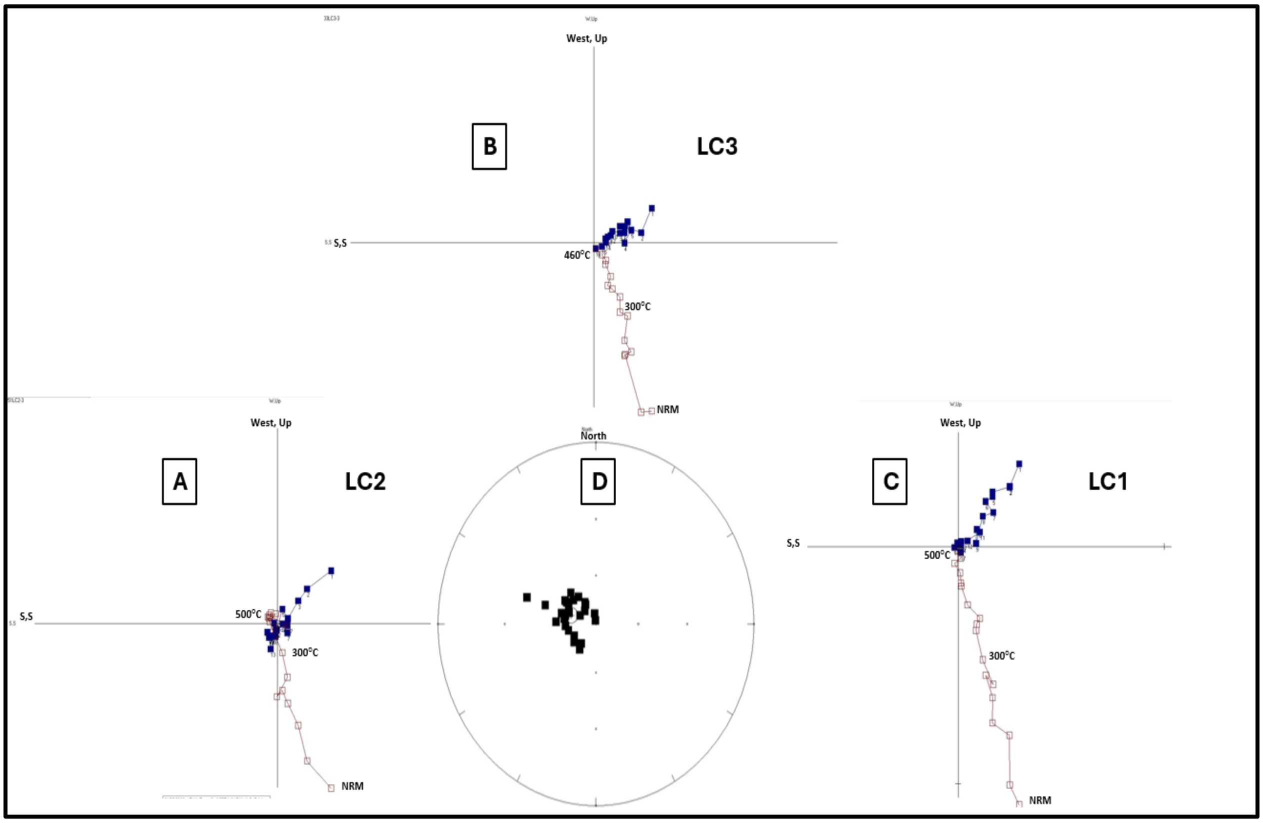

Figure 8: A-C) Orthogonal projection diagrams of representative samples of ChRM I at Lee's Canyon. Closed (open) circles represent horizontal (vertical) component of the magnetic component. D) Equal area plot of specimen directions of all samples that hold the first ChRM at Lee's Canyon. Closed (open) circles represent positive (negative) inclinations.

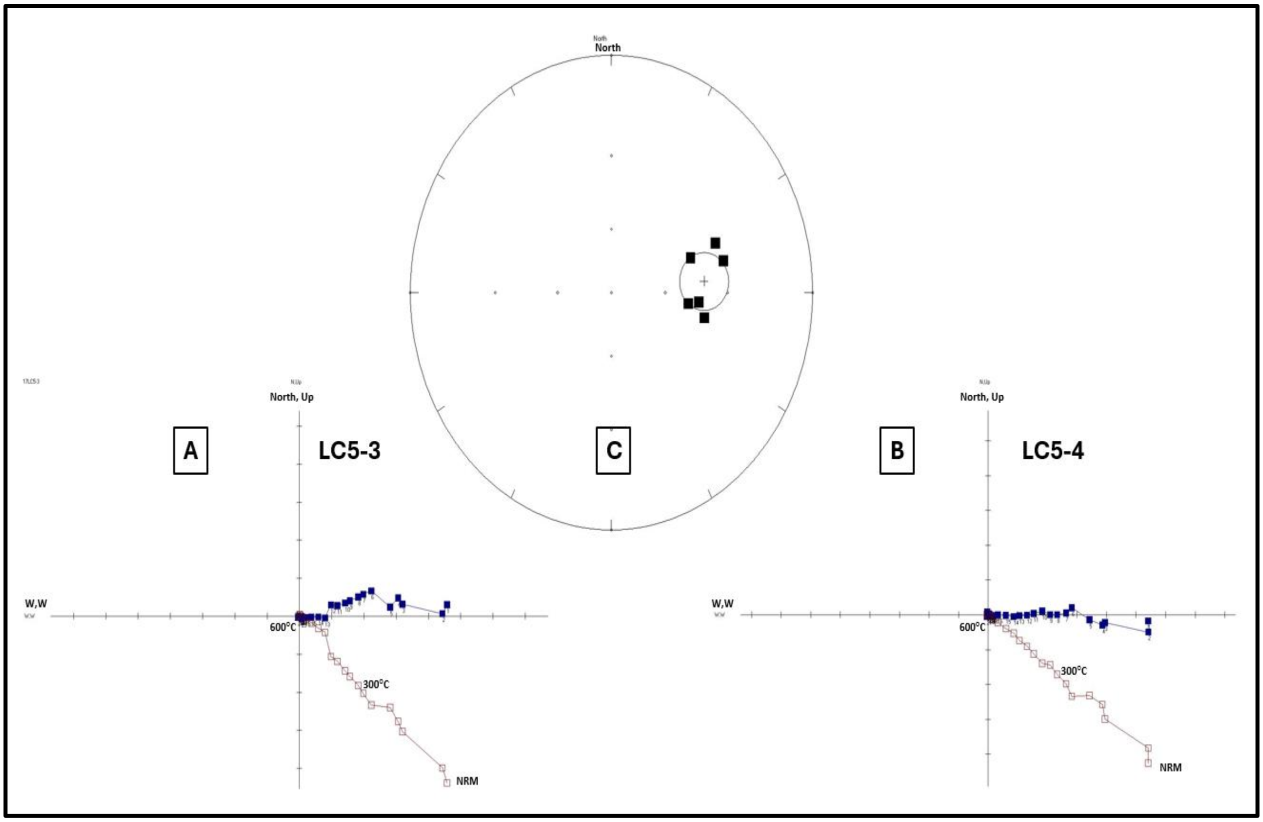

Figure 9: A-B) Orthogonal projection diagrams of representative samples of ChRM II at Lee's Canyon. Closed (open) circles represent horizontal (vertical) component of the magnetic components. D) Equal aera plot of specimen directions of all samples that hold the second ChRM at Lee's Canyon. Closed (open) circles represent positive (negative) inclinations.

Las Vegas Blvd.

The zebra dolomites collected from the Las Vegas Blvd. site were also sampled from the Mississippian Monte Cristo Formation. The zebra dolomite banding at Las Vegas Blvd. appears to be similar to the alternating bands of white saddle dolomite with light grey to dark bands of precipitated dolomite of similar thicknesses observed at Apex and Lee's Canyon. However, the samples have varying shades of pink to red mineralization.

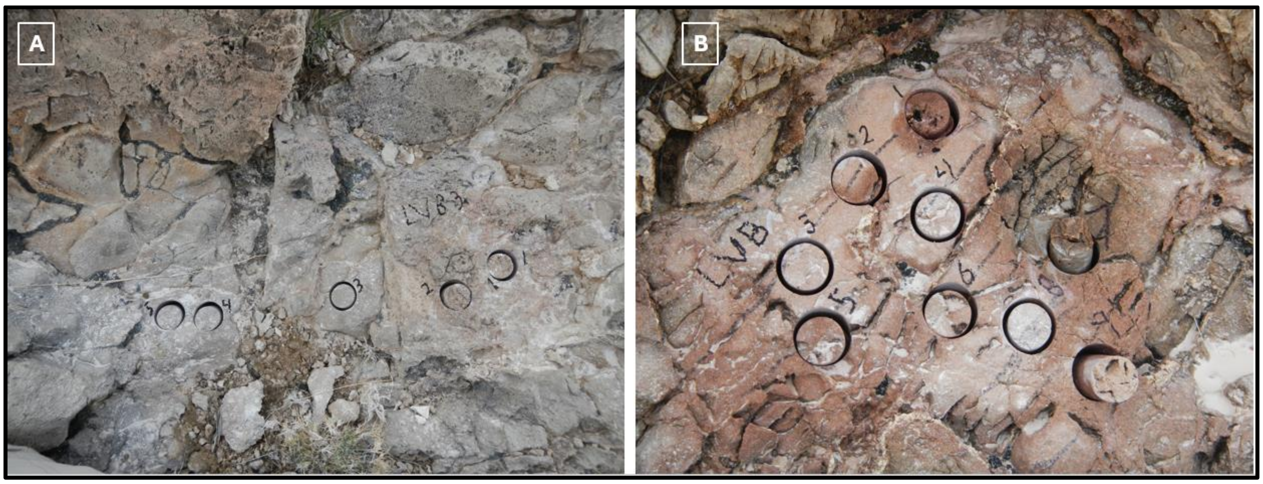

Figure 10: Zebra dolomite sampling sites from Las Vegas Blvd. location. Localized rhythmic bands of alternating dark replacement dolomite and white saddle dolomite. Red coloring is observed in samples at this location. A) Sample core removal from LVB1 site. B) Sample core removal from LVB2 site.

Thermal demagnetization at low temperatures (<200°C) removes a northerly and steep down component in many specimens (Figure 11 A-D). This is interpreted as the Modern VRM. At higher temperatures, the zebra dolomite at Las Vegas Blvd. holds a stable ancient magnetization. The characteristic remanent magnetization (ChRM) holds northwestern declinations and shallow negative inclinations and is removed between 580-660°C (Table 1). Shown in Figure 11 A-C are orthogonal projection diagrams for zebra dolomite specimens at Las Vegas Blvd. Figure 11 D highlights the equal area plot of specimen directions. The ChRM has unblocking temperatures of 580-660°C. This ChRM is found in all sample sites for the Las Vegas Blvd. zebra dolomites.

A mean direction was calculated for the ChRM component of the Las Vegas Blvd. zebra dolomites (Table 1). The *in situ* strike and dip of 175/52 was used as the correction for Cenozoic tilting for mean stratigraphic direction of the ChRM at LVB1 and LVB2 sample sites. The in-situ strike and dip of 188/40 was used as the correction at the LVB3 sample site. The mean stratigraphic direction of the ChRM in the zebra dolomite, corrected for Cenozoic extensional tilting, has a declination of 283.2°, with an inclination of -10.4° (k = 14.63, α95 = 8.4°; Table 1). At LVB sites, 71% of the specimens contain this ChRM. Specimens without the ChRM have low NRM intensities and only contain the VRM.

The stratigraphic mean of the zebra dolomite specimen directions was used to calculate a pole position for the ChRM found at Las Vegas Blvd. The calculated pole for the ChRM is at 7.5°N, 142.6°E (dp = 4.3°, dm = 8.5°) and the error ellipse intersects the Early Mississippian portion the apparent polar wander path (APWP) for North America (Figure 6).

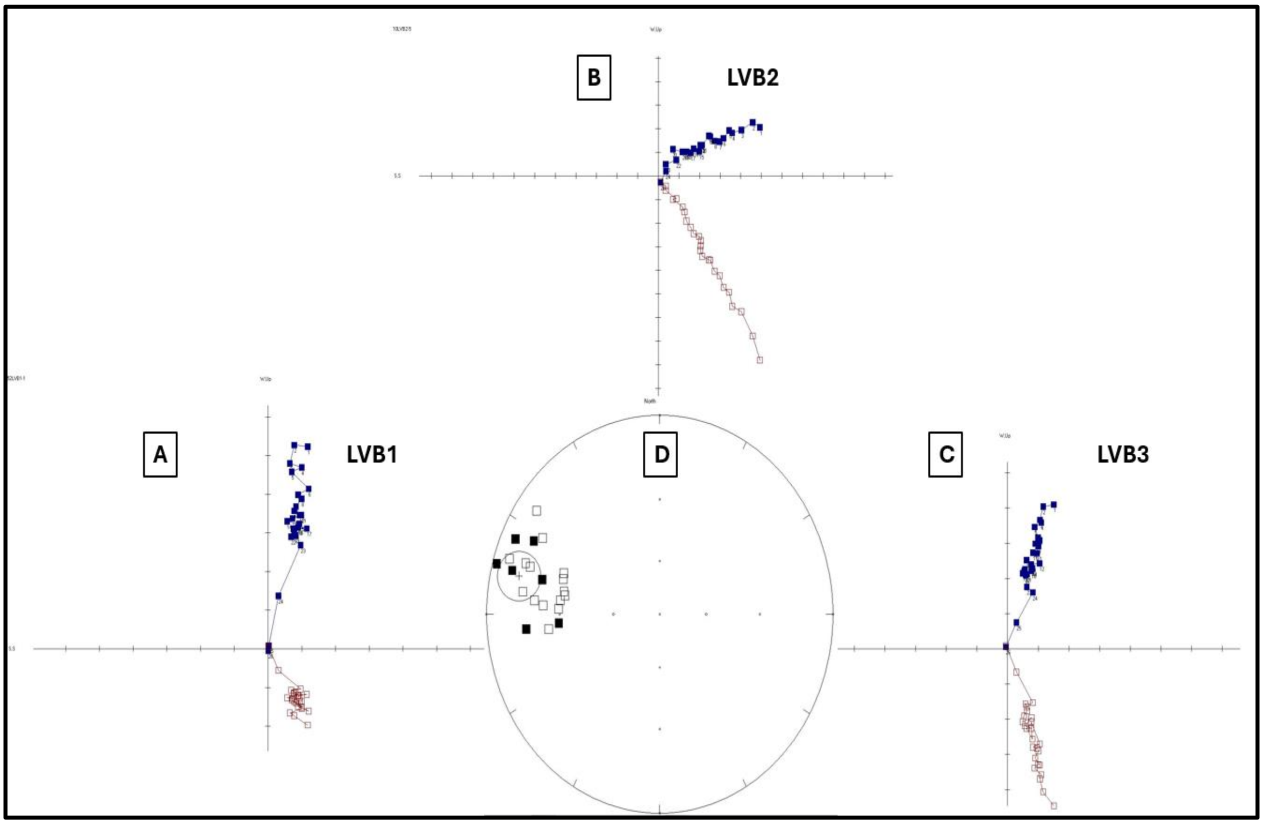

Figure 11: A-C) Orthogonal projection diagrams of representative samples of the ChRM at Las Vegas Blvd. Closed (open) circles represent horizontal (vertical) component of the magnetic component. D) Equal area plot of specimen directions of all samples that hold the ChRM at Las Vegas Blvd. Closed (open) circles represent positive (negative) inclinations

Central Nevada

Delamar Range

Zebra dolomites sampled from Delamar Range are from the Devonian Guilmette Formation. Zebra dolomites from this location display rhythmic banding of white saddle dolomite and black dolomite (~1-3mm band thickness) at a large stratigraphic interval as described by Dulin (2012).

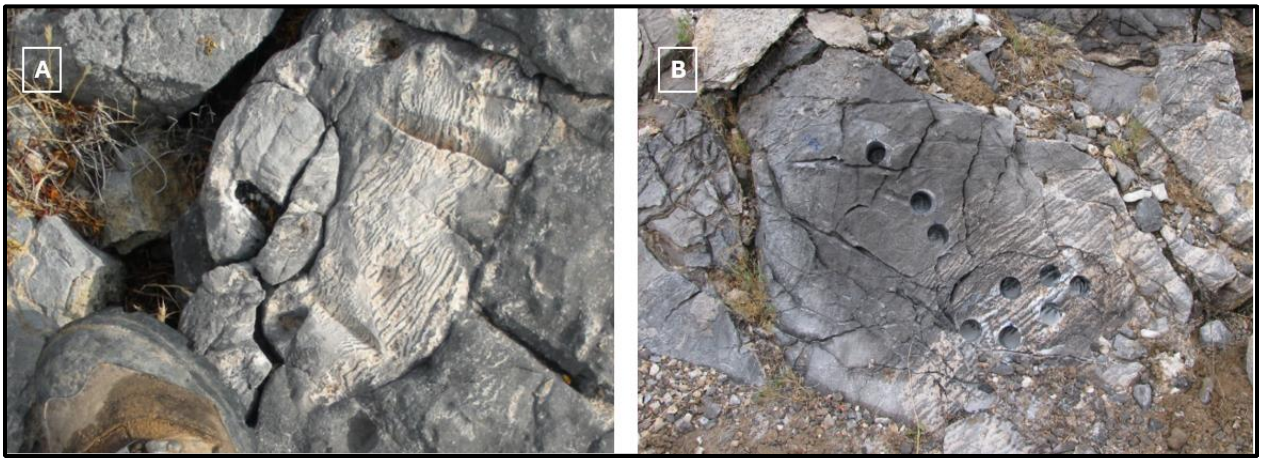

Figure 12: Zebra dolomite sampling sites from Delamar Range location. Localized rhythmic bands of alternating dark replacement dolomite and white saddle dolomite. A) Sample core removal from DZ1 site. B) Sample core removal from DZ2 site

Thermal demagnetization at low temperatures (<200°C) removes a northerly and steep down component in many specimens (Figure 13 A-B), interpreted as the Modern (VRM). At higher temperatures, the zebra dolomites sampled at Delamar Range have been remagnetized, however, it holds no stable ancient magnetizations. Shown in Figure 13 A-B are orthogonal projection diagrams for zebra dolomite specimens at Delamar Range. Figure 13C highlights the equal area plot of specimen directions. The random distribution of plotted points on the great circle provided no statistical trend to calculate a VGP pole position for this sample location, although samples held stable magnetizations. The ChRM has unblocking temperatures between 360°C-460°C.

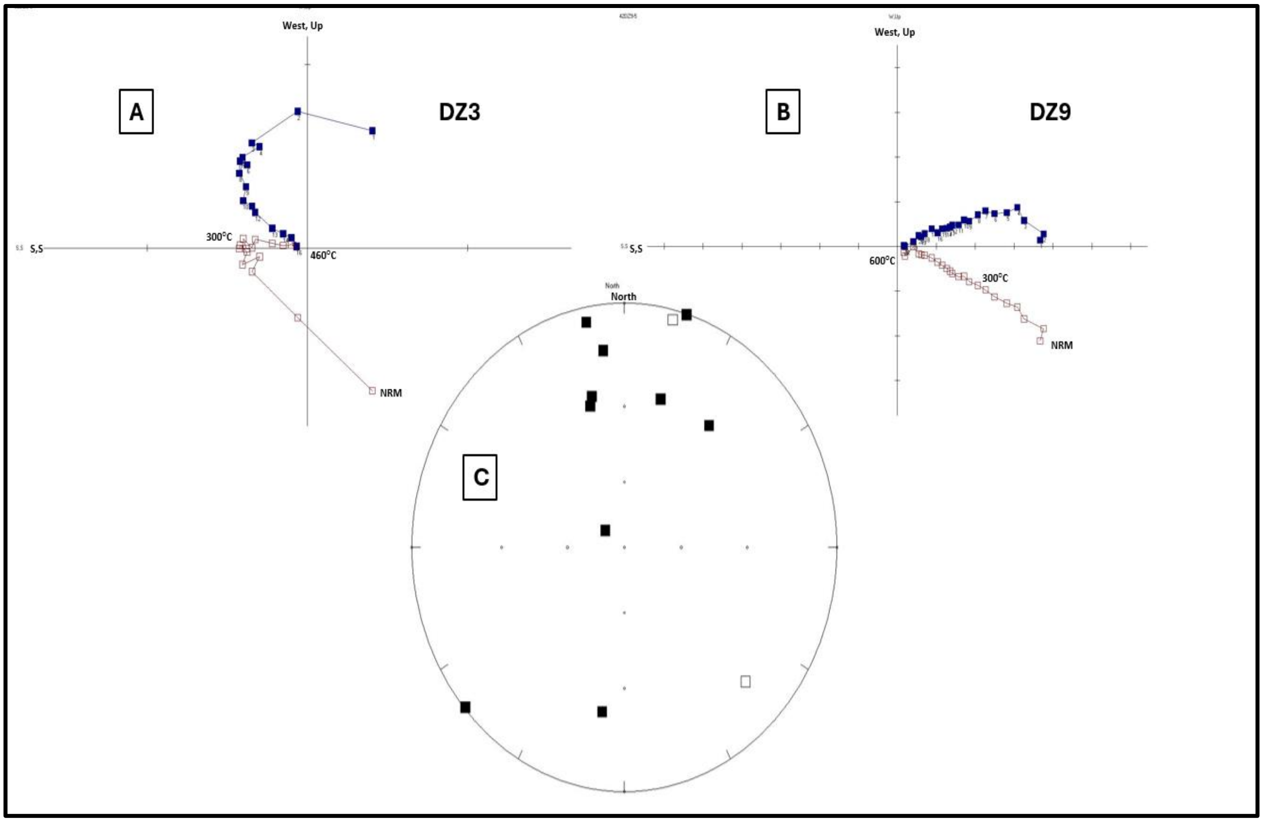

Figure 13: A-B) Orthogonal projection diagrams of representative samples of the ChRMs at Delamar Range. Closed (open) circles represent horizontal (vertical) component of the magnetic component. C) Equal area plot of specimen directions of all samples that hold the ChRMs at Delamar Range. Closed (open) circles represent positive (negative) inclinations.

Windfall

Zebra dolomites collected at the Windfall sample site were hosted in the Cambrian Windfall Formation. Zebra dolomites from this location are similar in appearance to samples from Delamar Range with large stratigraphic areas of alternating banding of white saddle dolomite and black dolomite. Windfall samples appear to have more frequent, and larger veins (2-10 mm banding thickness) of saddle dolomite compared to Delamar and Apex with also a very slight reddish color in the host dolomite (Figure 14 A-C). There were larger bands located at Windfall, with banding on the order of 1-3 meters thickness, although the location was not accessible to sample.

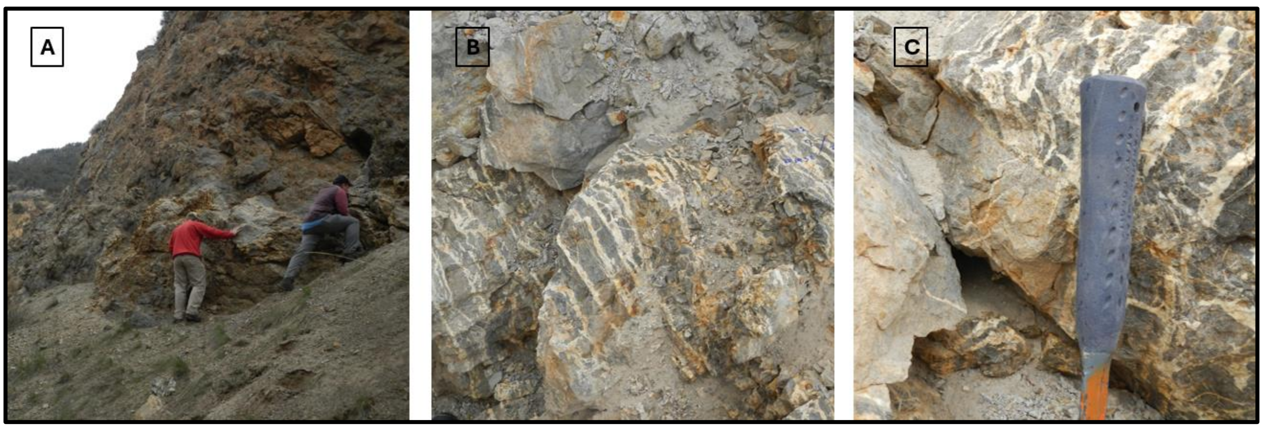

Figure 14: A) highlights the large stratigraphic area of zebra dolomites at Windfall sample site. B-C) highlights the rhythmic banding of zebra dolomites

Thermal demagnetization at low temperatures (<100°C) removes a northerly and steep down component in many specimens (Figure 15 A-C). This is interpreted as the Modern VRM. At higher temperatures, the zebra dolomite sampled at Windfall holds a stable ancient magnetization. However, due to sampling error, strike and dip were not recorded and therefore no Cenozoic tilting correction could be performed. Shown in Figure 15 A-B are orthogonal projection diagrams for zebra dolomite specimens at Windfall. Figure 15C highlights the equal area plot of specimen directions. The Windfall samples cluster together on the equal area plot with northeastern declinations and moderate inclinations. Again, due to error, no calculation of the VGP pole position for the Windfall location was performed. The magnetization held in these samples contained unblocking temperatures of 460°C.

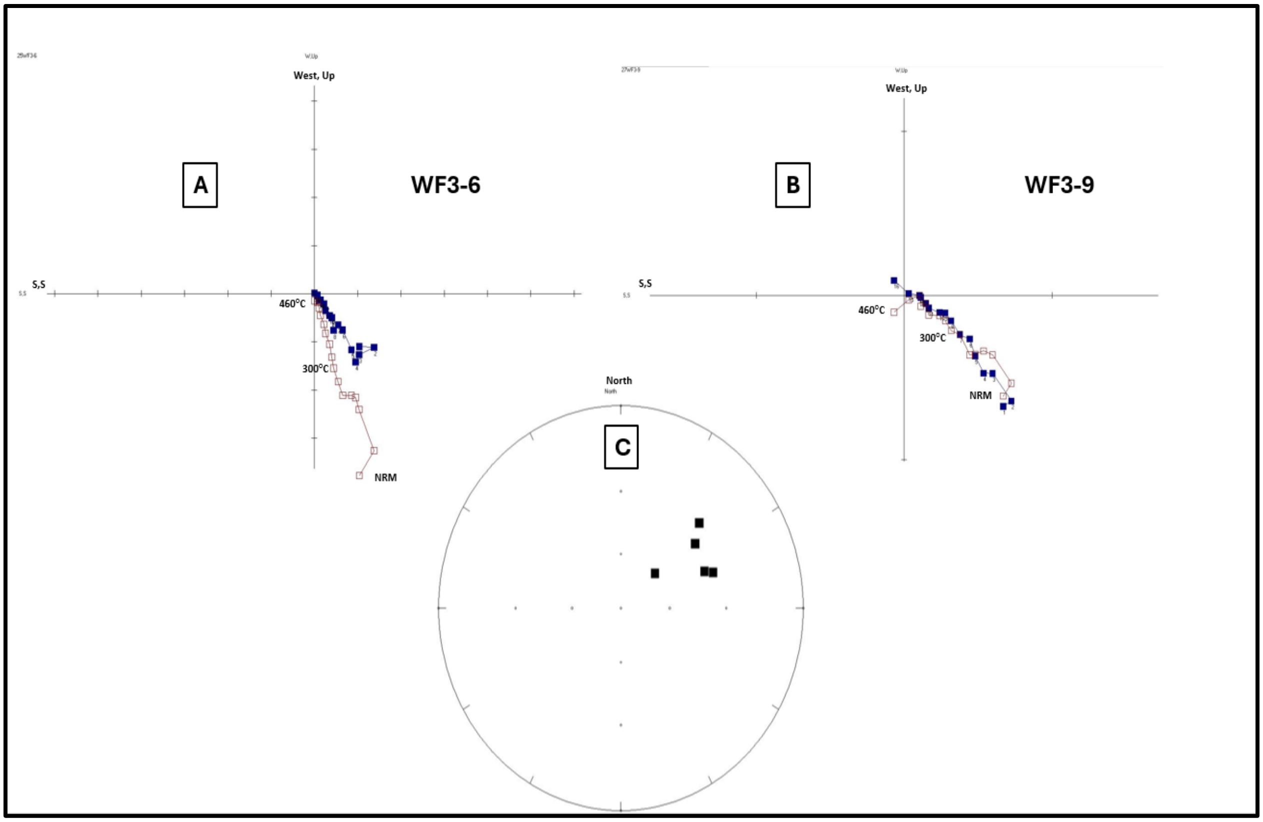

Figure 15: A-B) Orthogonal projection diagrams of representative samples of the ChRMs at Windfall. Closed (open) circles represent horizontal (vertical) component of the magnetic component. C) Equal area plot of specimen directions of all samples that hold the ChRMs at Windfall. Closed (open) circles represent positive (negative) inclinations

Ely

The zebra dolomites collected from the Ely site were sampled from the Permian Arcturus Formation. The zebra dolomites at Ely are predominantly comprised of light grey dolomite with numerous thin veins of white saddle dolomite throughout. Banding of saddle dolomite did not appear to be as pronounced as at the previous sample sites (Figure 16).

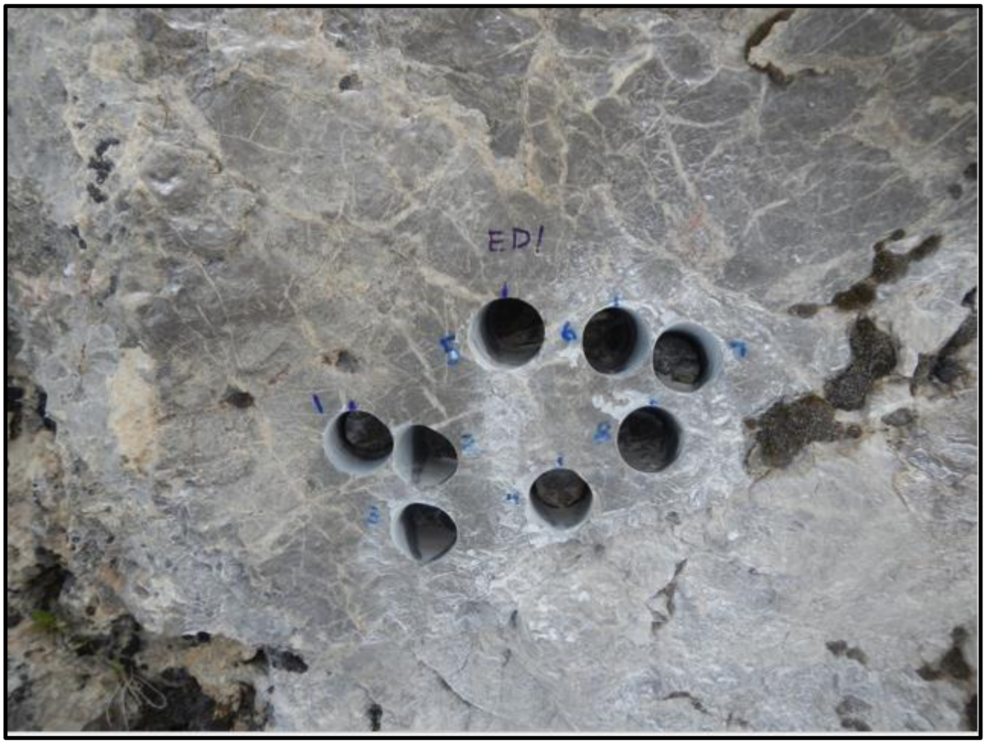

Figure 16: Highlights the fabric of zebra dolomites at site ED1. Hydrothermal saddle dolomite veins (less than 1 mm) were observed at the Ely location

Thermal demagnetization at low temperatures (<200°C) removes a northerly and steep down component in many specimens (Figure 17 A-C). This is interpreted as the Modern VRM. At higher temperatures, the zebra dolomite at Ely holds two stable ancient magnetizations. The first characteristic remanent magnetization (ChRM) holds northwestern declinations and steep inclinations and is removed between 480-600°C (Table 1). Shown in Figure 17 A-C are orthogonal projection diagrams for zebra dolomite specimens at Ely. Figure 17D highlights the equal area plot of specimen directions. This ChRM is found in 3 out of 4 sample sites for the Ely zebra dolomites.

The second ChRM holds north-northeastern declinations and moderate inclinations and is removed between 480-560°C (Table 1). Shown in Figure 18 A-B are orthogonal projection diagrams for the zebra dolomites of the second component. Figure 18C illustrates the equal area plot of the second component directions. The ChRM contains unblocking temperatures of 580°C. This ChRM was only found at the ED4 sample site.

Mean directions were calculated for both ChRM components of the Ely zebra dolomites (Table 1). The *in situ* strike and dip of 224/07 was used as the correction for Cenozoic tilting for mean stratigraphic direction of both ChRMs at Ely sample sites. The mean stratigraphic direction of the first ChRM in the zebra dolomite, corrected for Cenozoic extensional tilting, has a declination of 326°, with an inclination of 43.9° ($k = 26.31$, $\alpha 95 = 6°$; Table 1). At sites ED1-ED3, 85% of the specimens contain this first ChRM. The first ChRM is held within the majority of the 4 different ED sample sites. However, it is not present at ED4 (Table 1). Some of the specimens without the first ChRM have low NRM intensities and only contain the VRM.

The mean stratigraphic direction of the second ChRM in the zebra dolomite, corrected for Cenozoic extensional tilting, has a declination of 16.9°, with an inclination of 29.5° ($k = 1756.9$, $\alpha 95 = 1.8°$; Table 1). Again, *in situ* strike and dip of 224/07 was used as the correction for Cenozoic tilting for mean stratigraphic direction. At site ED4, 72% of the specimens contain the second ChRM. This ChRM is only found at the ED4 site.

The stratigraphic mean of the zebra dolomite specimen directions was used to calculate a pole position for each of the two ChRMs found at Ely. The calculated pole for the first ChRM is at 58.5°N, 139.8°E ($dp = 4.7°$, $dm = 7.5°$) and the error ellipse intersects the Middle Jurassic portion of the APWP (Figure 6). The calculated pole for the second ChRM is at 62.2°N, 151.9°E ($dp = 1.1°$, $dm = 2°$) and plots on the Middle-Late Jurassic portion of the path (APWP) for North America (Figure 6).

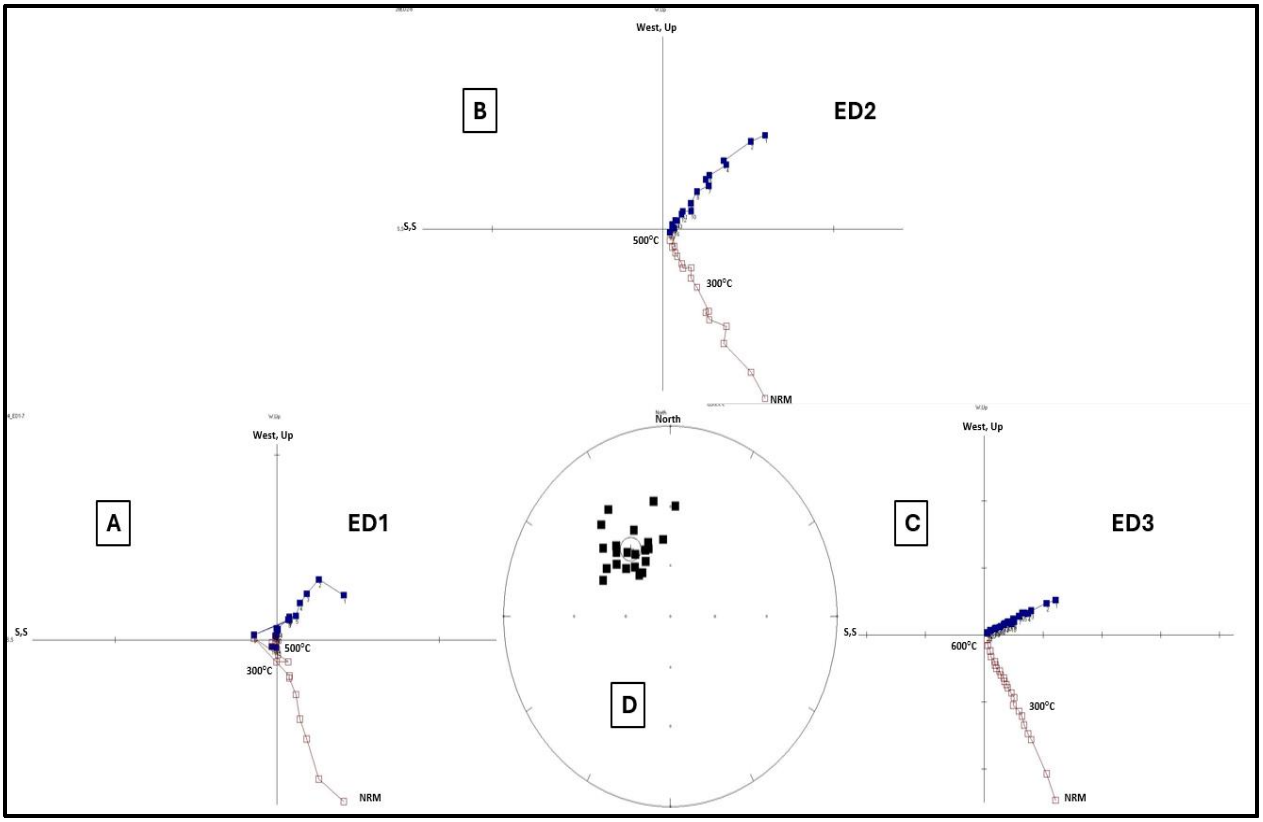

Figure 17: A-C) Orthogonal projection diagrams of representative samples of ChRM I at Ely. Closed (open) circles represent horizontal (vertical) component of the magnetic component. D) Equal area plot of specimen directions of all samples that hold the first ChRM at Ely. Closed (open) circles represent positive (negative) inclinations

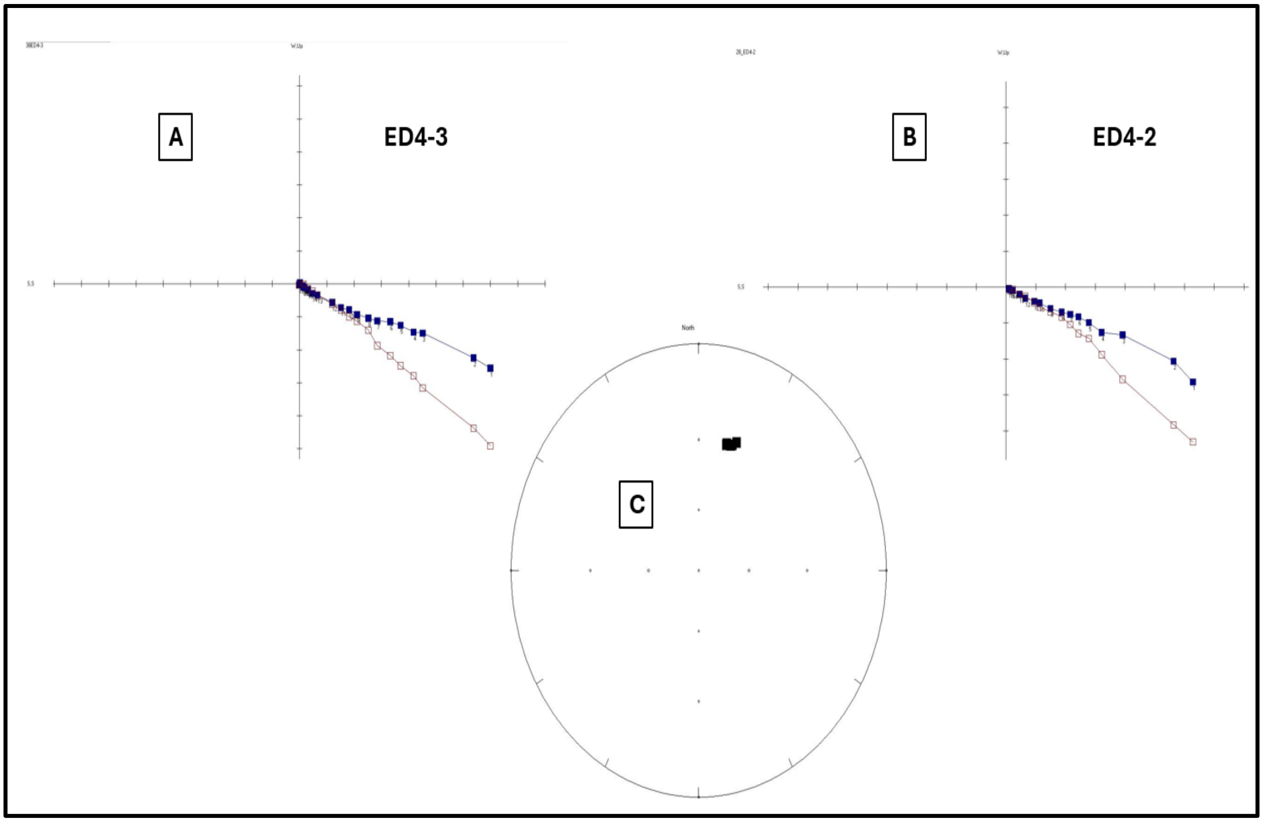

Figure 18: A-B) Orthogonal projection diagrams of representative samples of ChRM II at Ely. Closed (open) circles represent horizontal (vertical) component of the magnetic component. C) Equal area plot of specimen directions of all samples that hold the second ChRM at Ely. Closed (open) circles represent positive (negative) inclinations

Eureka

The zebra dolomites collected from the Eureka site were sampled from the Cambrian Hamburg Formation. The zebra dolomites at Eureka display alternating bands of white saddle dolomite with light grey to dark bands of precipitated dolomite of similar thicknesses (~2-3mm).

Thermal demagnetization at low temperatures (<200°C) removes a northerly and steep down component in many specimens (Figure 20 A-E). This is interpreted as the Modern VRM. At higher temperatures, the zebra dolomite at Eureka holds two stable components. Each ChRM component is plotted both geographically (without correction) and stratigraphically (with correction) due to uncertainties of the strike and dip of the EZD specimens at the sample locality (Figures 19, 20F, 21C). Geographically, the first characteristic remanent magnetization (ChRM) holds northwestern declinations and steep inclinations and is removed between 360-600°C (Table 1). Stratigraphically, the first characteristic remanent magnetization (ChRM) holds northeastern declinations and shallow inclinations and is removed between 400-600°C (Table 1).

Shown in Figure 20 A-E are orthogonal projection diagrams for zebra dolomite specimens at Eureka. Figure 20F highlights the stratigraphic equal area plot of specimen directions. This ChRM is found in all the sample sites for the Eureka zebra dolomites.

Geographically, the second ChRM holds northwestern declinations and shallow inclinations and is removed between 360-560°C (Table 1). Stratigraphically, the second ChRM holds northern declinations and shallow inclinations and is removed between 360-560°C (Table 1). Shown in Figure 21 A-B are orthogonal projection diagrams for the zebra dolomites of the second component. Figure 21C illustrates the stratigraphic equal area plot of the second component directions. This ChRM was only found at EZD1 and EZD7 sample sites (Table 1).

Mean directions were calculated for each of the two ChRM components of the Eureka zebra dolomites both geographically (without corrections) and stratigraphically (with Cenozoic corrections). (Table 1).

For the geographic direction, no strike and dip were used as a correction for Cenozoic tilting for the mean geographic direction of both ChRM components at Eureka sample sites due to inconsistencies with literature and geologic maps describing the Hamburg Formation near sampling sites EZD1-9. The mean geographic direction of the first ChRM in the zebra dolomite has a declination of 324.4°, with an inclination of 54° ($k = 24.72$, $\alpha95 = 4°$; Table 1). At sites containing first component, 83% of the specimens contain this first ChRM. The ChRM is held within the majority of the 9 different EZD sample sites. However, it is not present at EZD1, 6 & 7. All of the EZD6 specimens have low NRM intensities and plotted randomly on the equal area plots.

The mean geographic direction of the second ChRM in the zebra dolomite has a declination of 327.3°, with an inclination of 8.8° ($k =21.84$, $\alpha95 = 6.8°$; Table 1). The second ChRM is held only within EZD1 and EZD7 sample sites. At sites EZD1 and EZD7, 69% of the specimens contain this second ChRM.

The geographic mean of the zebra dolomite specimen directions was used to calculate a pole position for each of the two ChRMs found at Eureka. The calculated pole for the first ChRM is at 61.3°N, 155.4°E ($dp = 3.8°$, $dm = 5.5°$) and the error ellipse intersects the Middle Jurassic portion of the (APWP) for North America (Figure 6). The calculated pole for the second ChRM is at 44.2°N, 112.7°E (dp = 3.5°, dm = 6.9°) and intersects the Middle to Late Triassic portion of the (APWP) for North America (Figure 6).

Mean stratigraphic directions were also calculated for each of the two ChRM components found at the Eureka sample locality. The *in situ* strike and dip of 350/80 was used as the correction for Cenozoic tilting for mean stratigraphic direction of both ChRMs at Eureka sample sites. This value was chosen from a close geological map that provided a range of strike/dip values for the Hamburg dolomite near EZD sample locations (Long et al., 2014). The mean stratigraphic direction of the first ChRM in the zebra dolomite, corrected for Cenozoic extensional tilting, has a declination of 44.9°, with an inclination of 23° (k = 24.72, α95 = 4°; Table 1). At sites where the first EZD component is present, 83% of the specimens contain this first ChRM. The first ChRM is held within the majority of the 9 different EZD sample sites. However, it is not present at all in EZD1, 6, or 7.

The mean stratigraphic direction of the second ChRM in the zebra dolomite, corrected for Cenozoic extensional tilting, has a declination of 355.3°, with an inclination of 23.7° (k =21.84, α95 = 6.8°; Table 1). Again, *in situ* strike and dip of 350/80 was used as the correction for Cenozoic tilting for mean stratigraphic direction. At sites EZD1 and EZD7, 69% of the specimens contain the second ChRM. This ChRM is only found at the EZD1 and EZD7 sample sites.

The stratigraphic mean of the zebra dolomite specimen directions was used to calculate a pole position for each of the two ChRMs found at Eureka. The calculated virtual geomagnetic pole for the first ChRM is at 41.8°N, 176.1°E (dp = 2.7°, dm = 4.9°) and falls off of the (APWP) for North America (Figure 6). The calculated virtual geomagnetic pole for the second ChRM is at 62.6°N, 74°E (dp = 3.9°, dm = 7.3°) and the error ellipse intersects the Late Triassic/Early Jurassic portion of the (APWP) for North America (Figure 6).

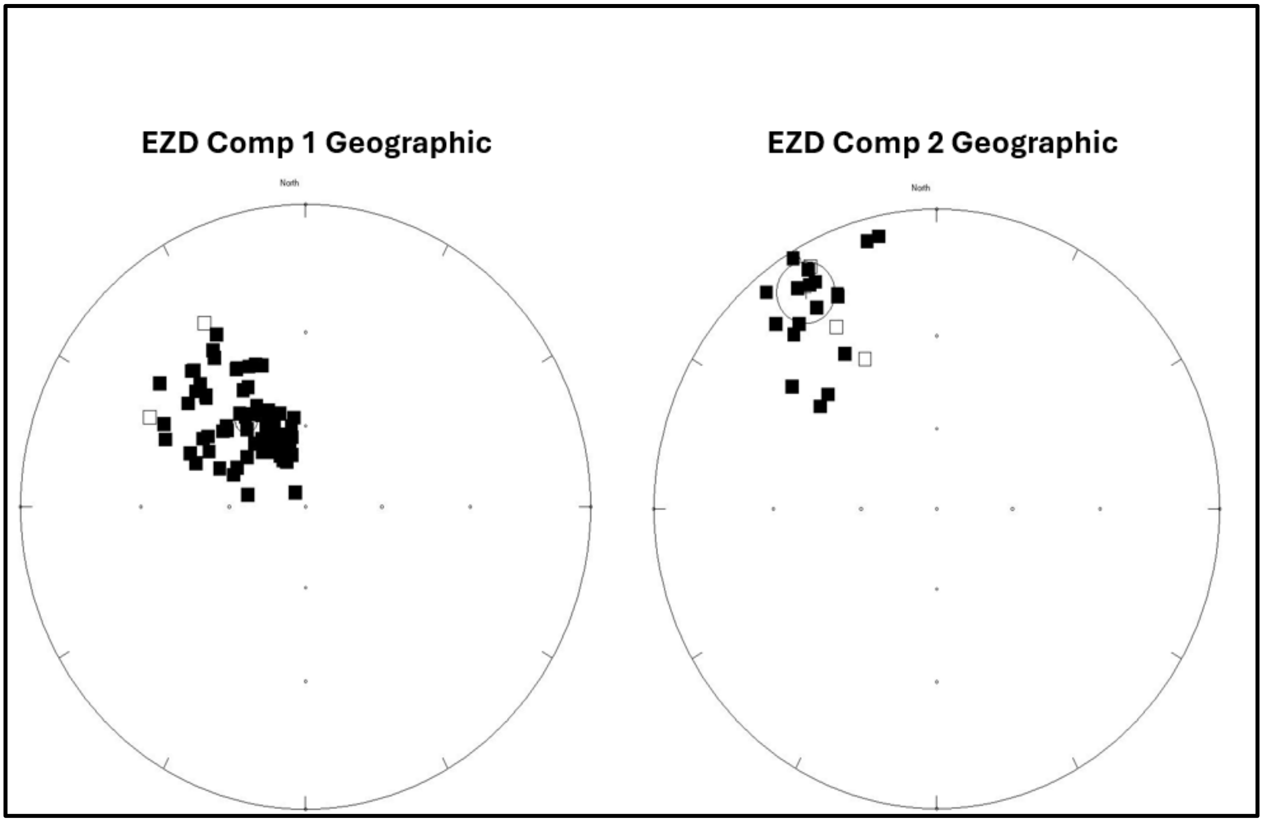

Figure 19: Equal area plots highlighting the geographic direction of the two different ChRMs held in EZD sample sites

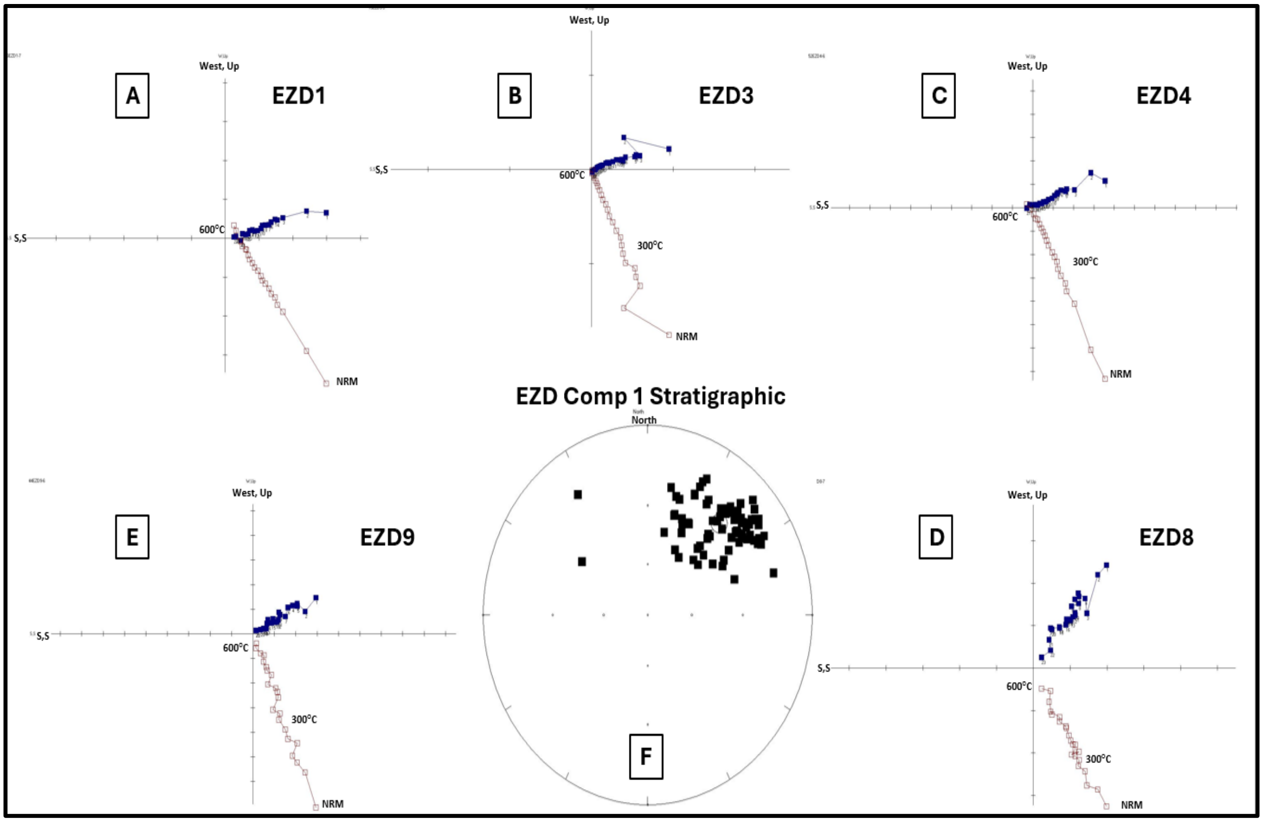

Figure 20: A-E) Orthogonal projection diagrams of representative samples of ChRM I at Eureka. Closed (open) circles represent horizontal (vertical) component of the magnetic component. F) Equal area plot of specimen stratigraphic directions of all samples that hold the first ChRM at Eureka. Closed (open) circles represent positive (negative) inclinations.

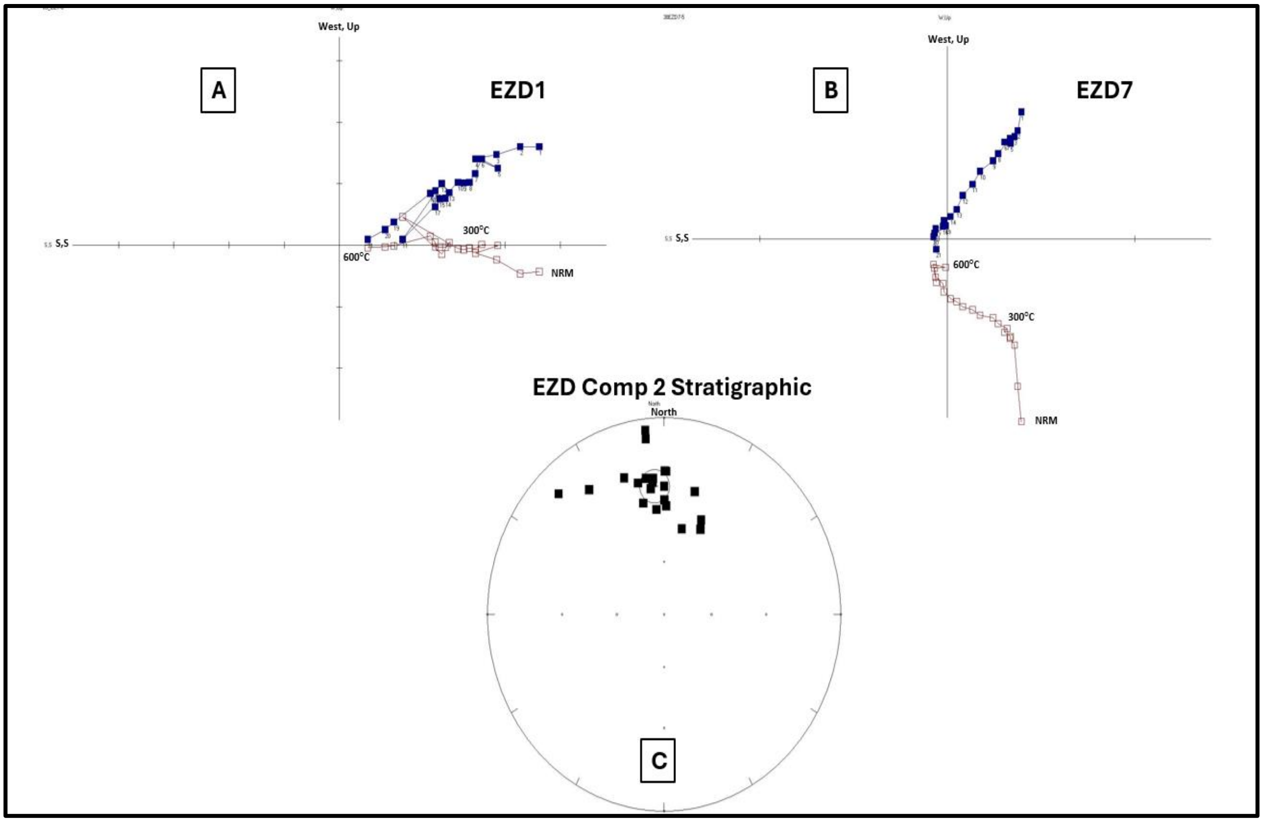

Figure 21: A-B) Orthogonal projection diagrams of representative samples of ChRM II at Eureka. Closed (open) circles represent horizontal (vertical) component of the magnetic component. C) Equal area plot of specimen stratigraphic directions of all samples that hold the second ChRM at Eureka. Closed (open) circles represent positive (negative) inclinations

Northern Nevada

Wendover

Additionally, zebra dolomites sampled from the Wendover (WZ) site are hosted in the Devonian Guilmette Formation on the eastern border of Nevada. Zebra dolomites from this location display rhythmic banding of white saddle dolomite and light grey dolomite with pink undertones. The zebra dolomite samples at Wendover contain much more white saddle dolomite than the previous locations. The Guilmette Formation host rock was heavily fractured and jointed with numerous white breccia masses at this location as described by Schneyer (1990).

Thermal demagnetization at low temperatures (<200°C) removes a northerly and steep down component in many specimens (Figure 22 A-B). This is interpreted as the Modern VRM. At higher temperatures, the zebra dolomite sampled at Wendover holds stable ancient magnetizations. Shown in Figure 22 A-B are orthogonal projection diagrams for zebra dolomite specimens at Wendover. Figure 22C highlights the equal area plot of specimen directions. The Wendover zebra dolomites cluster near the Modern declination and inclination for eastern Nevada (D=12°, I=63°). The magnetization held in these samples has unblocking temperatures of 460°C.

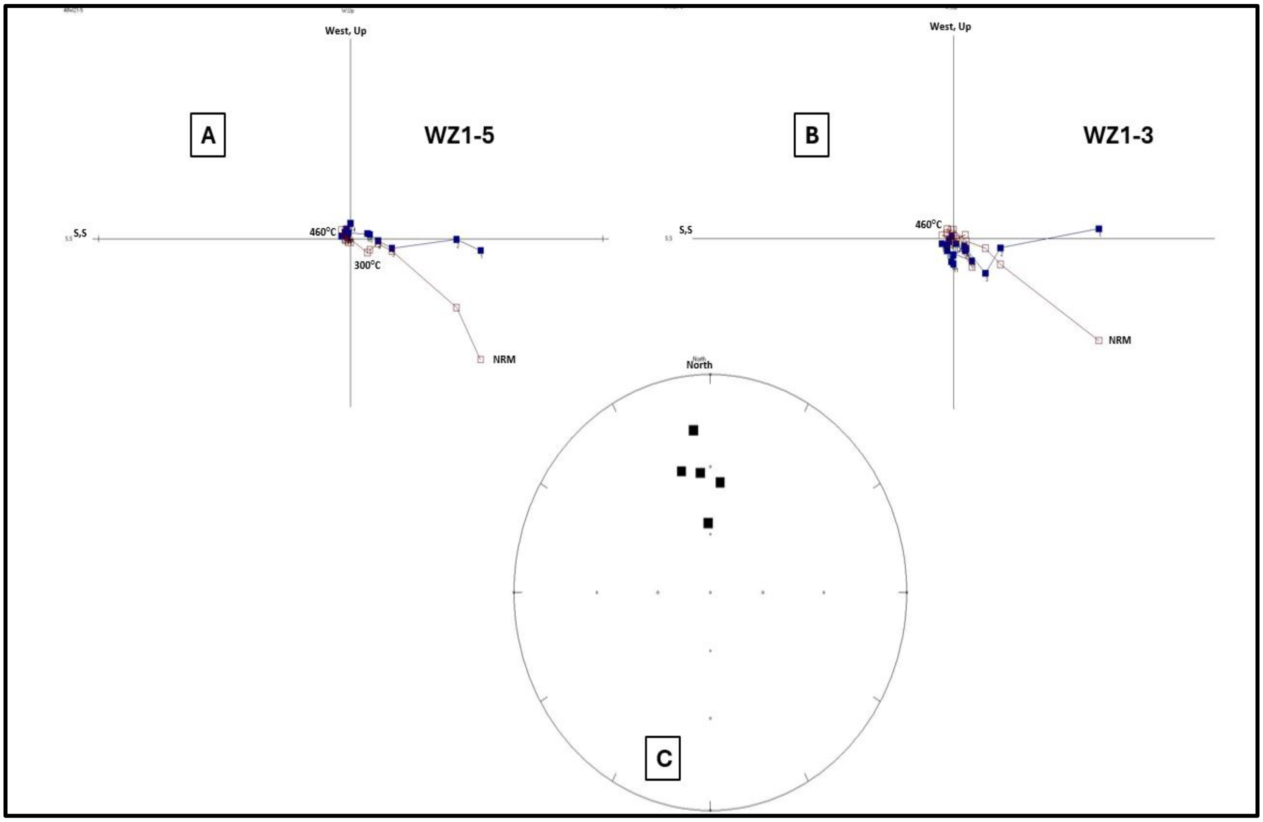

Figure 22: A-B) Orthogonal projection diagrams of representative samples of the ChRMs at Wendover. Closed (open) circles represent horizontal (vertical) component of the magnetic component. C) Equal area plot of specimen directions of all samples that hold the ChRMs at Wendover. Closed (open) circles represent positive (negative) inclinations.

Summit

The zebra dolomites collected from the Summit site were sampled from the Devonian Guilmette Formation. The zebra dolomites at Summit are predominantly comprised of white saddle dolomite with minimal grey host dolomite present at Summit sample sites.

Thermal demagnetization at low temperatures (<200°C) removes a northerly and steep down component in many specimens (Figure 23 A-B). This is interpreted as the Modern VRM. At higher temperatures, the zebra dolomite at Summit holds a stable ancient magnetization. The characteristic remanent magnetization (ChRM) holds northwestern declinations and steep inclinations and is removed between 400-480°C (Table 1). Shown in Figure 23 A-B are orthogonal projection diagrams for zebra dolomite specimens at Summit. Figure 23C highlights the equal area plot of specimen directions. This ChRM is found in all sample sites for the Summit zebra dolomites (Table 1).

A mean direction was calculated for the ChRM component of the Summit zebra dolomites (Table 1). The *in situ* strike/dip of 121/15 was used as the correction for Cenozoic tilting for mean stratigraphic direction of the ChRM at Summit sample sites. The mean stratigraphic direction of the ChRM in the zebra dolomite, corrected for Cenozoic extensional tilting, has a declination of 308.2°, with an inclination of 63.1° ($k = 57.15$, $\alpha95 = 12.3°$; Table 1). At SD sites, 80% of the specimens contain this ChRM. One of the specimens without the ChRM has low NRM intensities and only contains the VRM.

The stratigraphic mean of the zebra dolomite specimen directions was used to calculate a pole position for the ChRM found at Summit. The calculated pole for the ChRM is at 52.5°N, 178.6°E ($dp = 15.2°$, $dm = 19.4°$) and the error ellipse intersects the Late Jurassic portion of the (APWP) for North America (Figure 6).

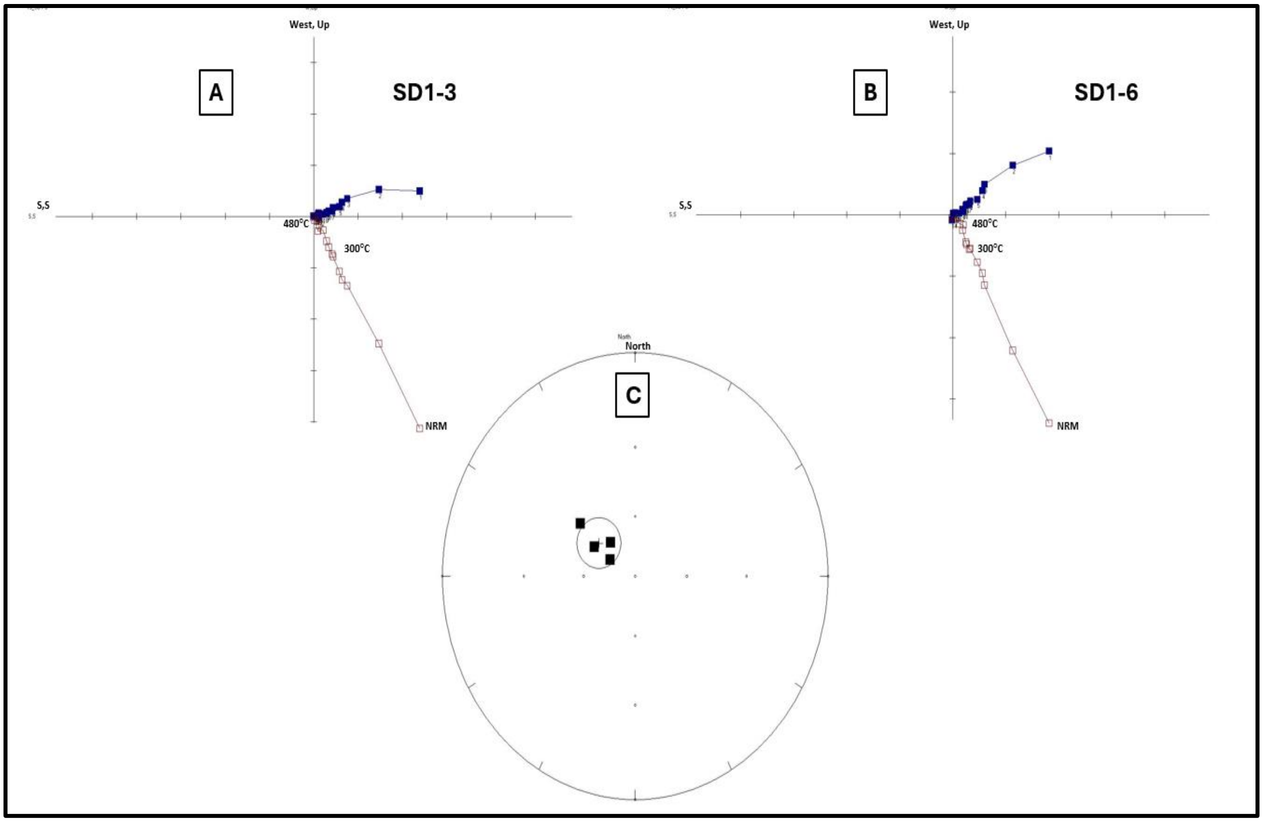

Figure 23: : A-B) Orthogonal projection diagrams of representative samples of the ChRM at Summit. Closed (open) circles represent horizontal (vertical) component of the magnetic component. C) Equal area plot of specimen directions of all samples that hold the ChRM at Summit. Closed (open) circles represent positive (negative) inclinations.

	Strike/Dip	N/N_0	Geo		*k*	α95	VGP	VGP	d_p(°)	d_m(°)	Strat		*k*	α95	VGP	VGP	d_p(°)	d_m(°)
			D(°)	*I(°)*			*Lat (°N)*	*Long (°E)*			*D(°)*	*I(°)*			Lat (°N)	Long (°E)		
EZD Comp 1																		
EZD2		4/6	336.5	51.7	88.03	13.4												
EZD3		15/16	330.4	66	68.86	4.6												
EZD4		15/21	330.1	45.7	29.66	7.1												
EZD5		5/7	333.4	60.2	141.05	6.5												
EZD8		9/9	320.1	41.4	45	7.8												
EZD9		8/8	297.8	54.4	42.14	8.6												
Mean		56/67	324.4	54.0	24.72	4	61.3	155.4	3.8	5.5	44.9	23	24.72	4	41.8	176.1	2.7	4.9
EZD Comp 2																		
EZD1		14/19	331.1	8	71.51	4.9												
EZD7		8/13	320.2	10.5	9.96	18.5												
Mean		*22/32*	*327.3*	*8.8*	*21.84*	*6.8*	*44.2*	*112.7*	*3.5*	*6.9*	*355.3*	*23.7*	21.84	6.8	62.6	74	3.9	7.3
AZ Comp 1																		
AZ1	136/11	7/9	330.7	59.2	36.71	10.1												
AZ2	136/11	7/10	334.5	58.8	34.06	10.5												
AZ3	136/11	6/8	332.8	57.9	100.64	6.7												
AZ4	136/11	1/4	344.8	58	99999	0												
AZ5	136/11	8/14	342.4	43.6	127.57	4.9												
AZ6	136/11	5/6	357.5	56.3	51.72	10.7												
AZ7	136/11	2/5	350.2	68.5	99999	0												
AZ8	320/04	11/12	338.1	52.2	93.12	4.8												
AZ10	136/11	12/12	313.5	52.3	19.68	10												
AZ12	136/11	11/14	330.6	48.4	41.66	7.2												
APQ2		2/2	345.3	39.1	907.94	8.3												
Mean		*72/96*	*333.9*	*53.5*	*30.69*	*3.1*					*318*	*55.7*	30.44	3	57.3	161.1	3.2	4.4
AZ Comp 2																		
AZ9	136/11	11/12	138.6	13.9	72.36	5.4												
AZ11	136/11	7/10	134.2	-1.8	46.22	9												
Mean	136/11	18/22	136.1	7	35.87	5.7					138.3	7.5	38.85	5.7	32.2	115.7	2.8	5.6

Table 1: Table showing statistics for all sites. Table marks whether statistics were calculated geographically or stratigraphically.

	Strike/Dip	N/N$_0$	Geo		*k*	α95	VGP	VGP	d_p(°)	d_m(°)	Strat		*k*	α95	VGP	VGP	d_p(°)	d_m(°)
LVB Comp 1			*D*(°)	*I*(°)											Lat (°N)	Long (°E)		
LVB1	175/52	8/11	280.8	26.1	29.84	10.3												
LVB2	175/52	8/12	293.8	34.8	23.63	11.6												
LVB3	188/40	6/8	279.6	51.4	24.83	13.7												
Mean		22/31	285.4	36.3	18.32	7.4					283.2	-10.4	14.63	8.4	7.5	142.6	4.3	8.5
ED Comp 1																		
ED1	224/07	5/6	318.9	58.9	71.32	9.1												
ED2	224/07	9/9	318.4	47.3	69.05	6.2												
ED3	224/07	9/12	341.5	48.2	19.26	12												
Mean	224/07	23/27	327.7	50.7	26.31	6					326	43.9	26.31	6	58.5	139.8	4.7	7.5
ED Comp 2																		
ED4	224/07	5/7	20.7	32.5	1756.9	1.8					16.9	29.5	1756.9	1.8	62.2	151.9	1.1	2
LC Comp 1																		
LC1	110/13	8/10	314.3	58.1	46.98	8.2												
LC2	110/13	5/5	315	65.3	197.29	5.5												
LC3	110/13	8/8	348.6	68	108.78	5.3												
LC4	110/13	5/9	280.2	79.6	195.68	5.5												
Mean	110/13	26/32	321.5	67.9	35.71	4.8					286.9	71.3	35.71	4.8	38.5	201.1	7.3	8.4
LC Comp 2																		
LC5	110/13	6/7	75.7	33.8	35.26	11.4					84.2	40.3	35.26	11.4	17.8	138.5	8.3	13.8
SD Comp 1																		
SD1	121/15	4/5	335.5	57.8	57.15	12.3					308.2	63.1	57.15	12.3	52.5	178.6	15.2	19.4

Table 2: Table showing statistics for all sites. Table marks whether statistics were calculated geographically or stratigraphically.

Microscopy and SEM

Twenty thin sections of the zebra dolomite were examined from the six study localities: EZD, LVB, AZ, LC, ED, and SD. The zebra dolomites are made up of alternating bands of white and black dolomites, with saddle dolomite being a common constituent. The banding does not manifest in thin section under plane polarized light, and a diffused light source must be used to identify the dark and light banding textures. There are scattered opaques seen throughout many of the thin sections with no discernable preferred orientations. In very few samples, it appears that the opaques are found in more abundance (though still very few) in the darker bands and not in the saddle dolomite.

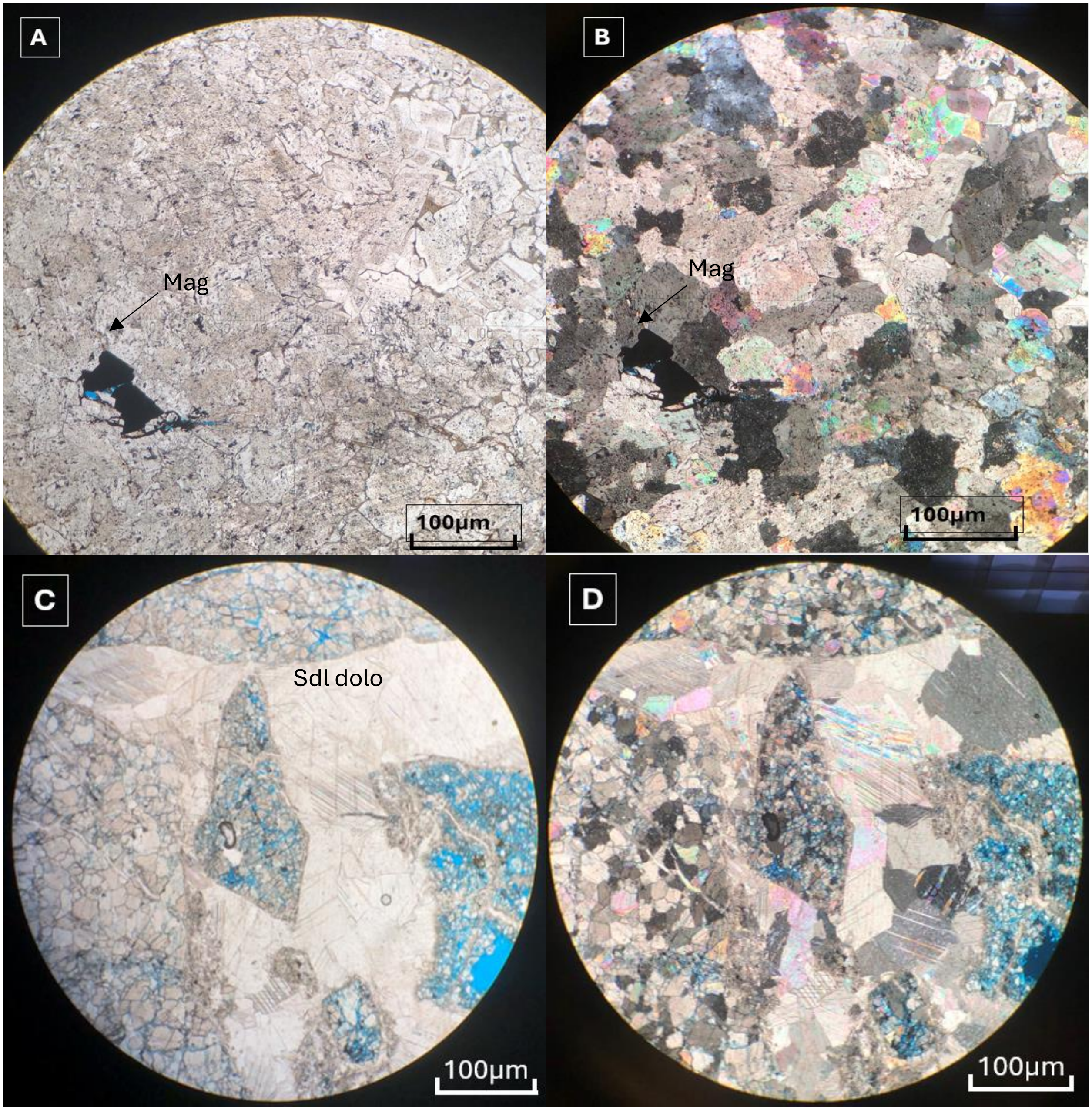

Figure 24: : Thin section samples of zebra dolomites in PPL vs. CPL. A) PPL thin section image of LVB1-4. B) CPL thin section image of LVB1-4. C) PPL thin section image of EZD4-11. D) CPL thin section image of EZD4-11. The zebra dolomite commonly shows the curved surfaces which indicate saddle dolomite. The color banding does not manifest in thin section.

Reflective light microscopy showed small, scattered reflective grains seen between the dolomite rhombs, with no preferential orientation for light or dark banding. The grains are interpreted as magnetite based on morphology (Figure 25). Some replacement of magnetite by hematite is seen within the dolomite, although it is rare. Figure 25A shows a reflective magnetite grain that is rimmed by hematite. The internal red reflection can be seen in the hematite alteration rim (Figure 25B).

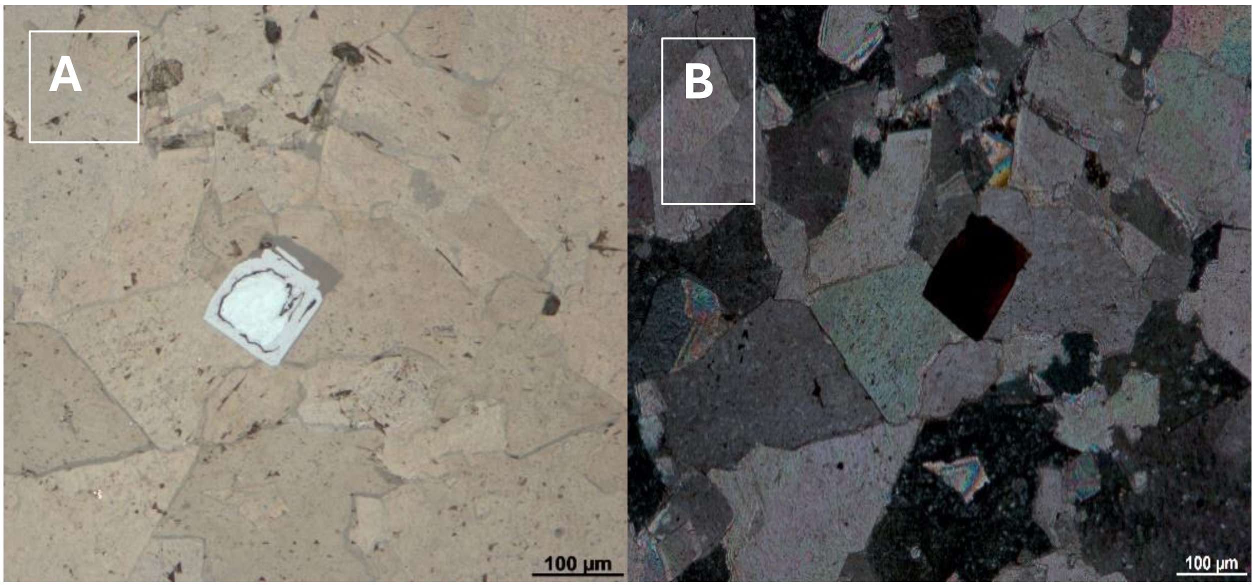

Figure 25: Magnetite grain altering to hematite. A) Reflective light showing magnetite grain with alteration rim and hematite replacement. B) CPL image showing red internal reflections of hematite.

Scanning electron microscopy was used to determine the habit of the magnetic minerals. The magnetization within the zebra dolomites is weak—on the order of 0.08mA/m or less—and the paucity of large magnetic grains made identification of potential remanence carriers difficult. Energy dispersive spectroscopy (EDS) detected high concentrations of iron. However, there appeared to be no preferential iron oxide habit (such as preferential differentiation in the light vs. dark bands).

Electron dispersive spectroscopy (EDS) analysis was performed on two specimens, EZD1-5 & ED3-7, from the Eureka and Ely zebra dolomite localities. Spectral maps of the zebra dolomite with shaded areas representing different elemental signatures with a supplemental table of the percentages of elemental signatures are shown in Figures 25-31.

Element	Atomic %	Atomic % Error	Weight %	Weight % Error
C	12.0	0.2	5.5	0.1
O	57.4	0.3	34.9	0.2
Na	0.6	0.1	0.5	0.1
Mg	2.0	0.1	1.8	0.1
Si	0.6	0.0	0.7	0.0
Ca	2.8	0.0	4.2	0.1
Fe	24.7	0.1	52.4	0.1

Figure 26 and Table 3: EDS spectral map of zebra dolomite from the Eureka site. Highlights interesting iron oxide habit within specimen EZD1-5. The table shows the elemental percentages of the EDS point on the iron oxide

The iron oxides present at one site within sample EZD1-5 are highlighted in Figure 26. The iron oxide is interpreted as magnetite based on morphology and elemental signatures.

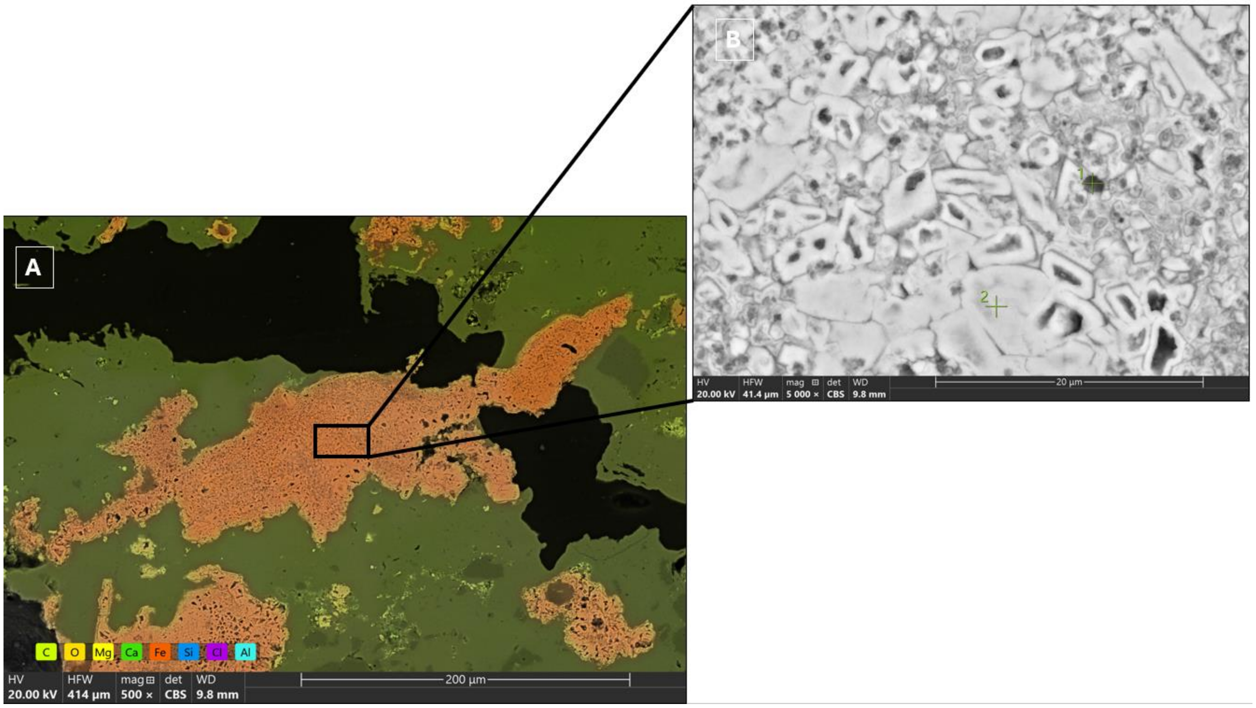

Element	Atomic %	Atomic % Error	Weight %	Weight % Error
C	12.8	0.2	4.7	0.1
O	39.9	0.2	19.4	0.1
Na	0.5	0.0	0.3	0.0
Mg	1.0	0.1	0.8	0.0
Al	0.3	0.0	0.3	0.0
Si	0.9	0.0	0.8	0.0
Cl	0.2	0.0	0.2	0.0
K	0.2	0.0	0.2	0.0
Ca	3.7	0.0	4.6	0.1
Fe	39.7	0.0	67.3	0.1

Figure 27 and Table 4: EDS spectral map of zebra dolomite from the Eureka site. Highlights a second interesting iron oxide habit within specimen EZD1-5. The table shows the elemental percentages of the EDS point on the iron oxide.

A large, elongated strip of iron oxides is depicted in Figure 27. Figure 27B highlights the interesting habit of the iron oxides. The table highlights the percentage of the elemental signatures analyzed. Based on the images of the iron oxides, it appears that they are precipitating within the void/vuggy porosity within the dolomite rhombs likely related to dolomitization.

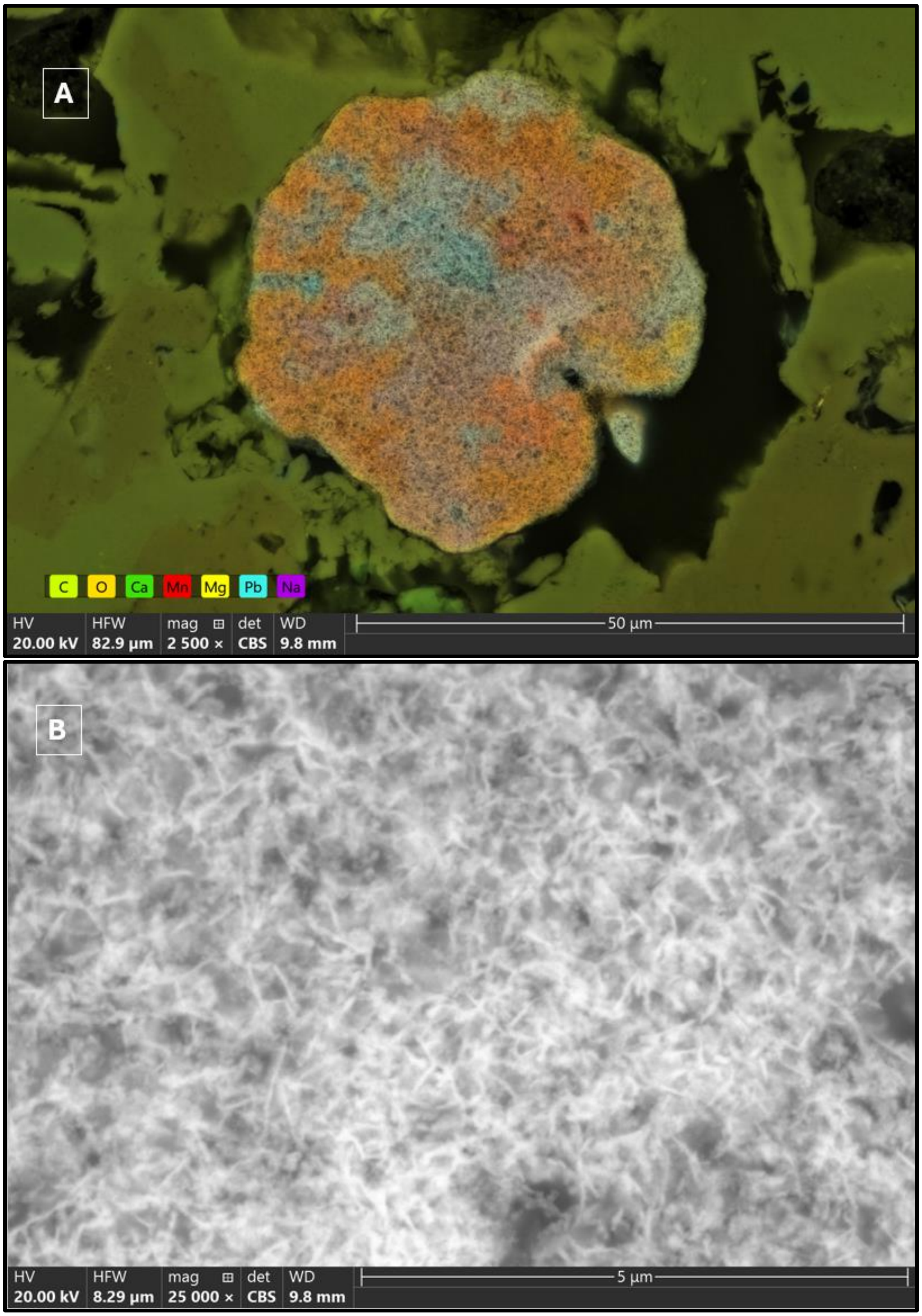

Element	Atomic %	Atomic % Error	Weight %	Weight % Error
C	35.7	0.2	19.0	0.1
O	45.5	0.2	32.2	0.2
F	0.0	---	0.0	---
Na	0.6	0.0	0.6	0.0
Mg	1.5	0.0	1.6	0.0
Al	0.3	0.0	0.4	0.0
Ca	4.4	0.0	7.8	0.0
Ti	0.1	0.0	0.3	0.0
Mn	8.8	0.0	21.3	0.1
Fe	1.7	0.0	4.2	0.1
Pb	1.4	0.0	12.6	0.2

Figure 28 and Table 5: : EDS spectral map of zebra dolomite from the Eureka site. Highlights another interesting iron oxide habit within specimen EZD1-5. The table shows the elemental percentages of the EDS point on the iron oxide. A) Spectral map highlighting Pb present in the iron oxide. B) Zoomed view of iron oxide with fibrous magnetite habit.

Another iron oxide held within EZD1-5 is highlighted in Figure 28. Again, the iron oxide appears to be precipitating within micro void/vuggy porosity of the dolomite rhombs. Smaller concentrations of Fe and an increase of Mn and Ti signatures were observed in this iron oxide. Lead (Pb) is present and is interesting because this confirms Diehl's (2010) hypothesis that ore deposits are associated with hydrothermal zebra dolomites near the Eureka Mining District and the associated lead deposits. A magnified view of the iron oxide is shown in Figure 28B. From the fibrous crystal habit displayed, this magnetic mineral is interpreted as fibrous magnetite.

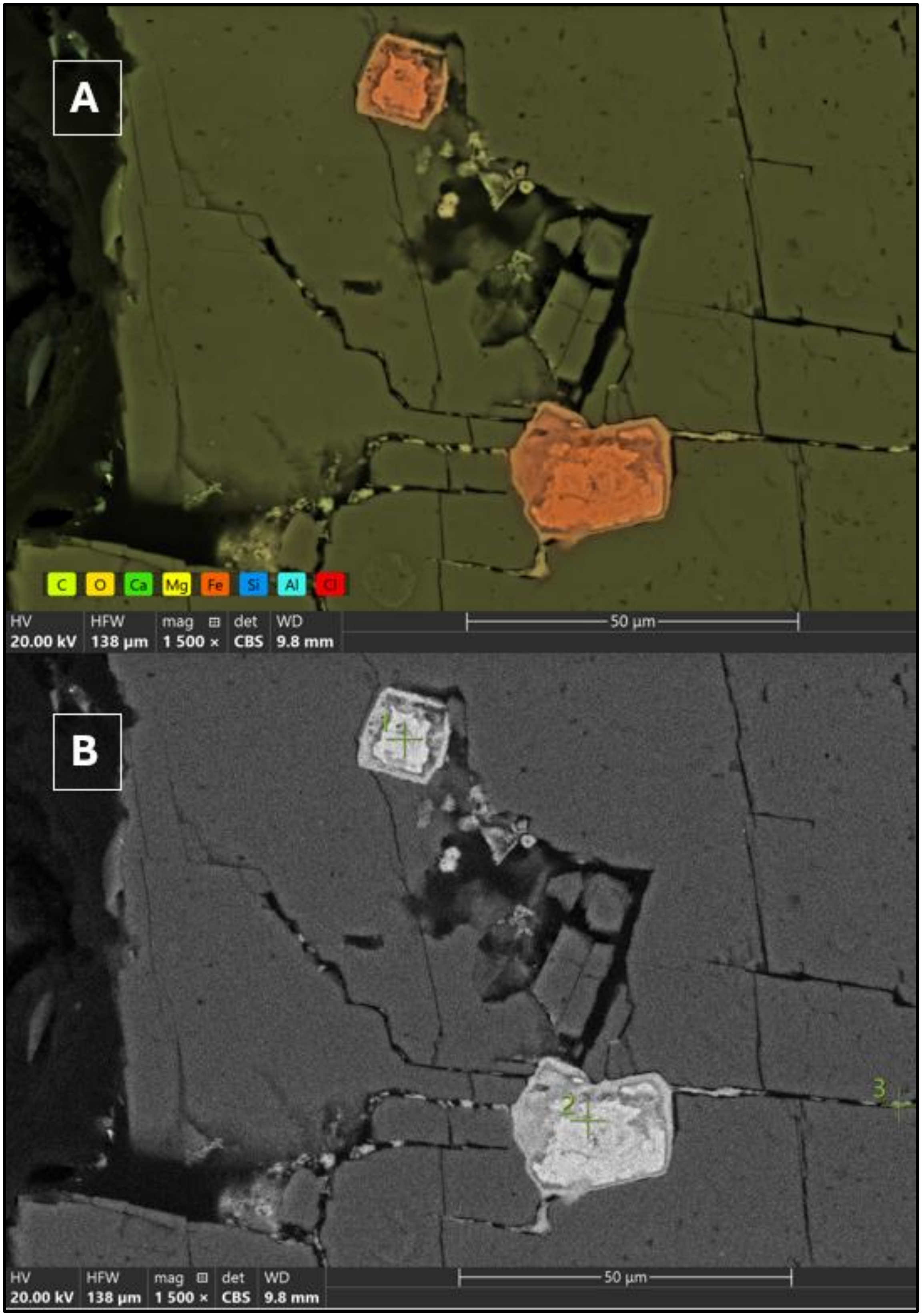
A
C
O
Ca
Mg
Fe
Si
Al
Cl
HV
20.00 kV
HFW
138 µm
mag
1 500 ×
det
CBS
WD
9.8 mm
50 µm
B
1
2
3
HV
20.00 kV
HFW
138 µm
mag
1 500 ×
det
CBS
WD
9.8 mm
50 µm

Point 1:

Element	Atomic %	Atomic % Error	Weight %	Weight % Error
C	7.8	0.1	3.7	0.0
O	63.6	0.2	40.4	0.1
Na	0.0	---	0.0	---
Mg	3.9	0.0	3.8	0.0
Al	0.4	0.0	0.4	0.0
Si	0.5	0.0	0.6	0.0
Ca	2.9	0.0	4.6	0.0
Fe	20.6	0.0	45.7	0.1
Zn	0.3	0.0	0.9	0.0

Point 2:

Element	Atomic %	Atomic % Error	Weight %	Weight % Error
C	8.2	0.1	3.7	0.0
O	59.0	0.2	35.6	0.1
Na	0.5	0.0	0.5	0.0
Mg	4.2	0.0	3.9	0.0
Al	0.4	0.0	0.4	0.0
Si	0.5	0.0	0.5	0.0
Ca	2.9	0.0	4.4	0.0
Fe	24.3	0.0	51.1	0.1

Point 3:

Element	Atomic %	Atomic % Error	Weight %	Weight % Error
C	12.4	0.1	6.7	0.0
O	60.5	0.2	43.7	0.2
Na	0.0	---	0.0	---
Mg	9.1	0.0	10.0	0.0
Al	0.7	0.0	0.8	0.0
Si	0.3	0.0	0.4	0.0
Ca	7.0	0.0	12.7	0.0
Fe	9.4	0.0	23.7	0.1
Zn	0.6	0.0	1.8	0.0

Figure 29 and Table 6: : EDS spectral map of zebra dolomite from the Eureka site. Highlights another square iron oxide habit within specimen EZD1-5. The table shows the elemental percentages of the EDS point on the iron oxide.

Another site of iron oxides present in EZD1-5 are displayed in Figure 29A-B. TheEDS was determined on 3 different points of the iron oxides. Points 1&2 contain relatively the same percentages of elemental signatures, dominated by Fe. However, Point 3 displays increased concentrations of Mg, Al, and Zn with a decrease in Fe compared to EDS values from Points 1&2. Also, Point 3 highlights the precipitation of iron oxides in void space between dolomite rhombs.

The EDS measurements were also made on specimen, ED3-7, from the Ely zebra dolomite locality. Figures 30-31 display spectral maps of the zebra dolomite with shaded areas representing different elemental signatures with supplemental tables of the percentages of elemental signatures.

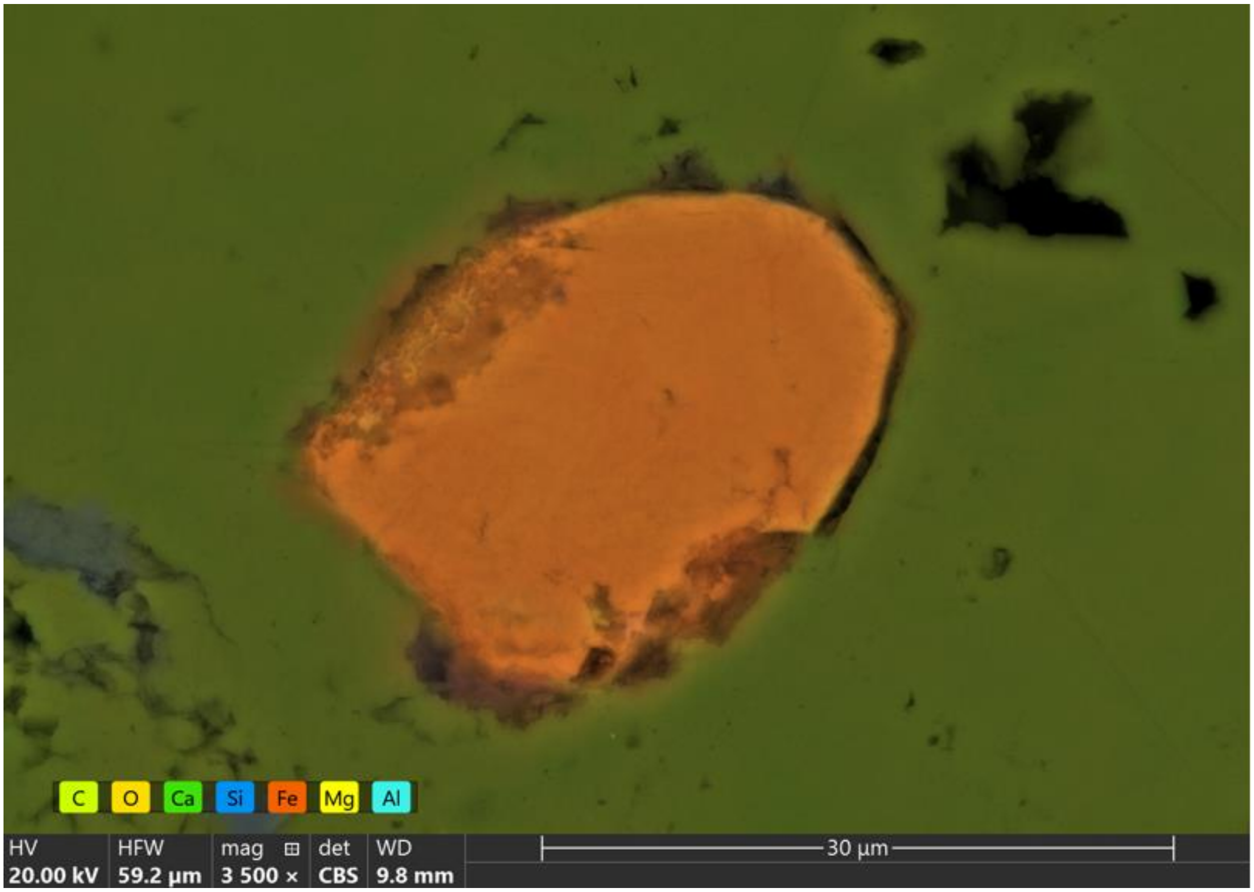

Element	Atomic %	Atomic % Error	Weight %	Weight % Error
C	4.4	0.1	2.0	0.0
O	64.9	0.3	39.3	0.2
Mg	0.3	0.0	0.2	0.0
Al	0.3	0.0	0.3	0.0
Si	2.4	0.0	2.5	0.0
S	0.1	0.0	0.1	0.0
Ca	4.6	0.0	6.9	0.1
Fe	23.0	0.1	48.6	0.1

Figure 30 and Table 7: EDS spectral map of zebra dolomite from the Ely site. Highlights an iron oxide habit within specimen ED3-7. The table shows the elemental percentages of the EDS point on the iron oxide.

One example of an iron oxide within ED3-7 is highlighted in Figure 30. This mineral is interpreted as magnetite due to high concentrations of Fe and habit. Compared to EZD1-5, specimen ED3-7 does not contain large concentrations of iron oxides. EZD1-5 had a natural remanent magnetization (NRM) intensity of 0.652 compared to sample ED3-7, which contained a NRM intensity of 0.324.

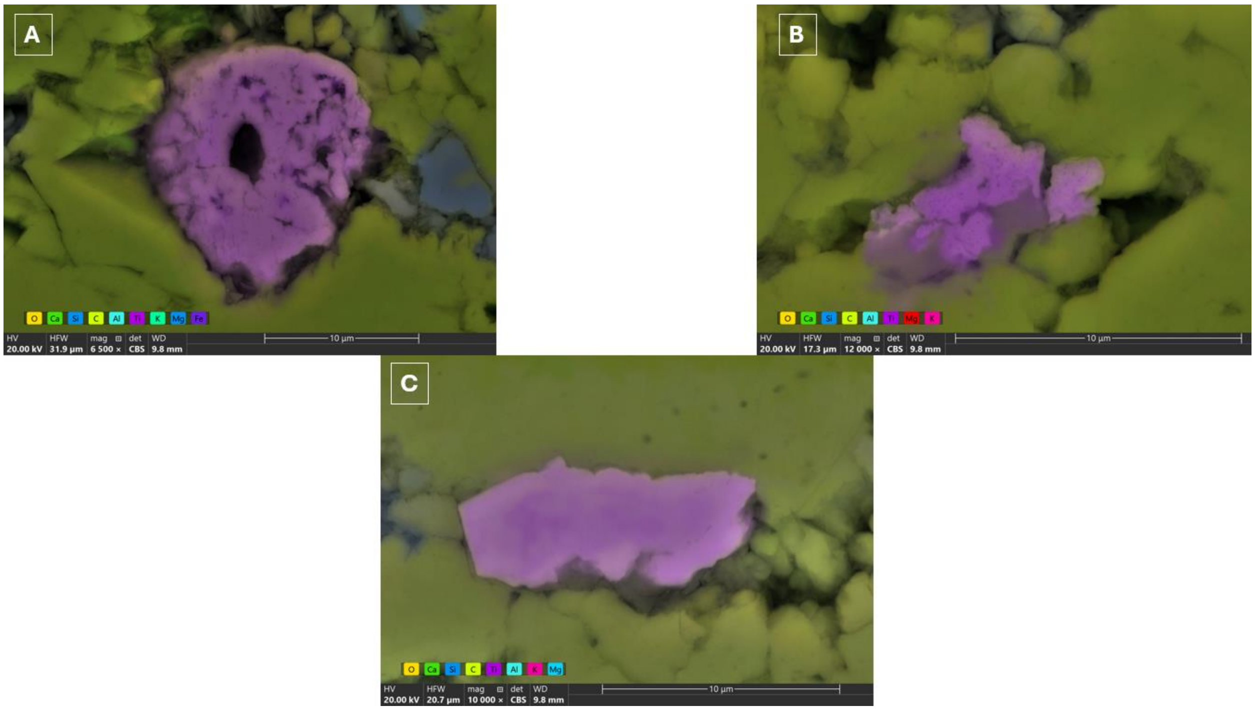

Table for A:

Element	Atomic %	Atomic % Error	Weight %	Weight % Error
C	4.6	0.1	2.3	0.0
N	9.2	0.4	5.4	0.2
O	58.8	0.4	39.5	0.3
Al	0.3	0.0	0.4	0.0
Si	1.2	0.0	1.4	0.0
Ca	3.9	0.0	6.6	0.0
Ti	21.7	0.1	43.8	0.1
Fe	0.2	0.0	0.6	0.0

Table for B:

Element	Atomic %	Atomic % Error	Weight %	Weight % Error
C	4.5	0.1	2.3	0.0
N	9.1	0.4	5.4	0.2
O	58.1	0.4	38.9	0.3
Mg	0.1	0.0	0.2	0.0
Al	0.3	0.0	0.4	0.0
Si	1.3	0.0	1.5	0.0
K	0.1	0.0	0.2	0.0
Ca	4.5	0.0	7.6	0.1
Ti	21.8	0.1	43.7	0.1

Table for C:

Element	Atomic %	Atomic % Error	Weight %	Weight % Error
C	3.9	0.1	2.1	0.0
N	7.5	0.3	4.6	0.2
O	63.0	0.4	44.0	0.3
Mg	0.2	0.0	0.2	0.0
Al	0.5	0.0	0.6	0.0
Si	1.8	0.0	2.2	0.0
K	0.1	0.0	0.2	0.0
Ca	5.2	0.0	9.1	0.1
Ti	17.4	0.1	36.4	0.1
Fe	0.2	0.0	0.6	0.0

Figure 31 and Table 8: EDS spectral map of zebra dolomite from the Ely site. Highlights an iron oxide habit within specimen ED3-7. The table shows the elemental percentages of the EDS points on the iron oxide

The iron oxides present throughout ED3-7 are represented by Figure 30 A-C. These iron oxides have an increased concentration of Ti compared to the iron oxides present in sample EZD1-5. Iron oxides observed in sample ED3-7 form in the interstitial pore space in between dolomite rhombs. Based on habit of the iron oxides and the elemental signatures within, these minerals are interpreted to be titanomagnetite and hold the magnetization present in the ED3-7 specimen.

DISCUSSION

Southern Nevada

Apex

Two ChRMs are observed in zebra dolomite specimens from the Apex sample site. The zebra dolomites were sampled from the Mississippian Monte Cristo Formation. Specific burial temperature data for the Monte Cristo Fm in Nevada are limited. Clumped isotope analysis of fluid inclusions in the over lying Bird Spring Formation provided maximum burial temperatures of 100-165°C (Shenton et al., 2015). Therefore, the Mississippian Monte Cristo Formation likely experienced similar if not slightly higher burial temperatures.

The *in situ* strike and dip of 136/11 was used as the correction for Cenozoic tilting for mean stratigraphic direction of both ChRMs at Apex sample sites. Although there is evidence of counterclockwise vertical axis rotation throughout the Basin and Range Province, no correction was used. Vertical axis rotation resulting from Cenozoic tectonics, range from 90° in the western portion of the state to no rotation in parts of eastern Nevada and are too far away from sampling locations to be interpolated to the Apex study area (Hudson et al., 2000; McQuarrie & Wernicke, 2005; Best et al., 2013; Petronis et al., 2014).

The mean stratigraphic direction of the first ChRM in the zebra dolomite, corrected for Cenozoic extensional tilting, has a declination of 318°, with an inclination of 55.7° ($k = 30.44$, $\alpha95 = 3°$; Table 1). The mean stratigraphic direction of the second ChRM in the zebra dolomite, corrected for Cenozoic extensional tilting, has a declination of 138.3°, with an inclination of 7.5° ($k = 38.85$, $\alpha95 = 5.7°$; Table 1). The first mean direction in the zebra dolomite is similar to Late Paleozoic directions found throughout Nevada (Gillett and Karlin, 2004). Gillett and Karlin (2004) determined that the tilting post-dated the acquisition of the Paleozoic aged magnetizations throughout Nevada. Although no tilt test was performed (due to lack of opposing dips in stratigraphic interval of interest), it is likely that the ChRM was acquired prior to Cenozoic Basin and Range extension.

The first ChRM held within the mineralized zebra rocks has a VGP that plots on the Middle to Late Jurassic portion of the APWP. The first ChRM is observed in all but two sampling sites. The second ChRM is only held within sample sites AZ9 & AZ11 and has a VGP that intersects the Pennsylvanian portion of the APWP. Due to unblocking temperatures below 580°C, both ChRMs are interpreted to be held in magnetite. Based on the relatively low burial temperatures, and the time-temperature relaxation time curves for single domain (Pullaiah et al., 1975) and multidomain (Kent, 1985; Middleton and Schmidt, 1982) magnetite, both ChRMs are interpreted as CRMs. The presence of two ChRMs within this area may be related to porosity differences due to fracture-related fluid migration networks.

The first CRM held in the zebra dolomite is interpreted as a remagnetization derived from hydrothermal fluids that are related to the Central Nevada Thrusting. These hydrothermal fluids are interpreted to have been transported through previous existing faults and fractures in the area related to earlier tectonics such as the Sonoma Orogeny.

The second CRM in the zebra dolomite at Apex is interpreted as an early remagnetization from the Pennsylvanian that likely is a product of hydrothermal fluids expelled during the final stages of the Antler Orogeny, tectonic stresses from the Ancestral Rockies, or other localized tectonics.

Las Vegas Blvd.

A ChRM is observed in zebra dolomite specimens from the Las Vegas Blvd. sample site. The zebra dolomites were also sampled from the Mississippian Monte Cristo Formation. Zebra dolomites at LVB contain varying shades of red mineralization that differs from samples at Apex. This red colored mineralization is interpreted as hematite. Specific burial temperature data for the Monte Cristo Fm in Nevada are limited. Clumped isotope analysis of fluid inclusions in the over lying Bird Spring Formation provided maximum burial temperatures of 100-165°C (Shenton et al., 2015). Therefore, the Mississippian Monte Cristo Formation likely experienced similar if not slightly higher burial temperatures.

The *in situ* strike and dip of 175/52 was used as the correction for Cenozoic tilting for mean stratigraphic direction of the ChRM at LVB1 & LVB2 sample sites and 188/40 at LVB3 sample site. Although there is evidence of counterclockwise vertical axis rotation throughout the Basin and Range Province, no correction was used. Vertical axis rotation resulting from Cenozoic tectonics, range from 90° in the western portion of the state to no rotation in parts of eastern Nevada and are too far away from sampling locations to be interpolated to the Las Vegas Blvd. study area (Hudson et al., 2000; McQuarrie & Wernicke, 2005; Best et al., 2013; Petronis et al., 2014).

The mean stratigraphic direction of the ChRM in the zebra dolomite, corrected for Cenozoic extensional tilting, has a declination of 283.2°, with an inclination of -10.4° ($k = 14.63$, $\alpha 95 = 8.4°$; Table 1). The ChRM held within the mineralized zebra rocks has a VGP that plots on the Early Mississippian portion of the APWP. The ChRM is observed in all sampling sites at LVB. Due to unblocking temperatures between 580-660°C, the ChRM is interpreted to be held in magnetite and/or maghemite. The unblocking temperature is 645°C and is interpreted as a CRM.

The CRM in the zebra dolomite at Las Vegas Blvd. is interpreted as an early remagnetization from the Early Mississippian that is a product of hydrothermal fluids expelled during the initial stages of the Antler Orogeny.

Lee's Canyon

Two ChRMs are observed in zebra dolomite specimens from the Lee's Canyon sample site. The zebra dolomites were sampled from the Cambrian Nopah Formation. The Nopah Formation experienced burial due to sediment accumulation and the Antler and Sevier orogenies. While specific temperature ranges for the Nopah are not well documented, studies of similar Cambrian carbonate formations in Nevada suggest that burial temperatures likely ranged from 100-200°C based on general geothermal gradients and the thickness of overlying sediments (Ekren, 1971; Carr, 1988; Diehl et al., 2010). It is interpreted that samples from Lee's Canyon likely experienced similar burial temperatures and depths.

Although there is evidence of counterclockwise vertical axis rotation throughout the Basin and Range Province, no rotational correction was used. Vertical axis rotation resulting from Cenozoic tectonics, range from 90° in the western portion of the state to no rotation in parts of eastern Nevada and are too far away from sampling locations to be interpolated to the Lee's Canyon study area (Hudson et al., 2000; McQuarrie & Wernicke, 2005; Best et al., 2013; Petronis et al., 2014).

The mean stratigraphic direction of the first ChRM in the zebra dolomite, corrected for Cenozoic extensional tilting, has a declination of 286.9°, with an inclination of 71.3° ($k = 35.71$, $\alpha95 = 4.8°$; Table 1). The mean stratigraphic direction of the second ChRM in the zebra dolomite, corrected for Cenozoic extensional tilting, has a declination of 84.2°, with an inclination of 40.3° ($k = 35.26$, $\alpha95 = 11.4°$; Table 1). The first ChRM held within the mineralized zebra rocks has a VGP that falls off of the APWP. The first ChRM is observed in all sampling sites except for LC5. The second ChRM is only held within the LC5 sample site and has a VGP that intersects the Silurian portion of the APWP. Due to unblocking temperatures below 580°C, both ChRMs are interpreted to be held in magnetite. Based on the relatively low burial temperatures, and the time-temperature relaxation time curves for single domain (Pullaiah et al., 1975) and multidomain (Kent, 1985; Middleton and Schmidt, 1982) magnetite, both ChRMs are interpreted as CRMs.

The first CRM in the zebra dolomite at Lee's Canyon is interpreted as a younger remagnetization that likely is a product of hydrothermal fluids expelled during one of the many tectonic events that characterized Nevada. It is interpreted that the first CRM does not plot near the APWP due to perceived localized block rotation near the Lee's Canyon sampling site. Again, due to extreme variations in values for vertical axis rotation, no specific value could be applied with confidence.

The second CRM in the zebra dolomite at Lee's Canyon is interpreted as an early remagnetization from the Silurian that either formed due to diagenesis during shallow burial remagnetization and/or precipitation of authigenic hematite and magnetite growth due to hydrothermal fluid influence. Authigenic magnetite is present in thin sections as opaques filling voids or vugs in the specimens.

Central Nevada

Delamar Range

Zebra dolomites from the Devonian Guilmette Formation located in the Delamar Range likely experienced maximum burial temperatures from 150-350°C based on the Conodont Alteration Index (CAI) values published by the United States Geological Survey (1989). However, it is noted that at one collection location, the CAI was estimated to be as low as 3.0 (Karklins et al., 1989). This maximum burial temperature is similar to the values Dulin (2014) reported for the Guilmette Fm. Dulin (2014) observed a southerly and shallow stable CRM held in magnetite at Delamar Range. This remagnetization is consistent with paleomagnetic studies of carbonate rocks in Nevada (Evans et al., 2012) (Gillett & Karlin, 2004). Dulin (2014) found that the entirety of the Guilmette Formation at Delamar Range has been remagnetized and the stable remagnetization plots on the Late Pennsylvanian portion of the APWP.

Results from Delamar Range in this study indicate that zebra dolomite specimens contain remagnetizations. However, when grouped on the equal area plot, the distribution of points is random and no calculation of a VGP was able to be produced. The random distribution of stable magnetizations observed in specimens from Delmar Range sample sites are interpreted to be associated with numerous pulses of hydrothermal fluids from differing tectonic events that followed previous planes of weakness in the Guilmette Formation. The stable magnetizations are interpreted to be held in titanomagnetite based on unblocking temperatures between 360-460°C. The scattering of the data are likely due to the widely scattered sampling sites of zebra dolomite within the Delamar Range. These samples were taken from discrete zebra locations, not large, bedded zebra dolomites, which may explain the random distribution of data for these collections of samples.

Windfall

Zebra dolomites collected from the Windfall sample site are hosted in the Cambrian Windfall Formation. Zebra dolomites from this location are similar in appearance to samples from Delamar Range with large stratigraphic areas of alternating banding of white saddle dolomite and black dolomite. Thermal history data on Cambrian aged rocks in central Nevada indicate that Cambrian rocks experienced temperatures ranging from 110-200°C based on research of the Late Cretaceous upper-crustal thermal structure of the Sevier hinterland (Blackford et al., 2021).

At Windfall sample sites, a stable ChRM was observed at WF3. The Windfall samples cluster together on the equal area plot with northeastern declinations and moderate inclinations. However, due to sampling error during collection, no calculation of the VGP pole position for the Windfall location was performed. The magnetization held in these samples is interpreted to reside in titanomagnetite based on unblocking temperatures of 460°C. Resampling of the Windfall zebra dolomites and their surrounding host rock could yield conclusive paleomagnetic data that would assist in dating the remagnetization and explain the localized tectonics and fluid flows at this locality.

Ely

Two ChRMs are observed in zebra dolomite specimens from the Ely sample site. The zebra dolomites were sampled from the Permian Arcturus Formation. Determination of precise burial temperatures for the Arcturus Formation is challenging due to limited direct thermal data. Therefore, it is reasonable to assume that the Arcturus likely reach burial temperatures less than or near 200°C, compared to the other Paleozoic carbonates in the area of study.

Although there is evidence of counterclockwise vertical axis rotation throughout the Basin and Range Province, no correction was used. Vertical axis rotation resulting from Cenozoic tectonics, range from 90° in the western portion of the state to no rotation in parts of eastern Nevada and are too distant from sampling locations to be interpolated to the Ely study area (Hudson et al., 2000; McQuarrie & Wernicke, 2005; Best et al., 2013; Petronis et al., 2014).

Mean directions were calculated for both ChRM components of the Ely zebra dolomites. The mean stratigraphic direction of the first ChRM in the zebra dolomite, corrected for Cenozoic extensional tilting, has a declination of 326°, with an inclination of 43.9° ($k = 26.31$, $\alpha 95 = 6°$; Table 1). The mean stratigraphic direction of the second ChRM in the zebra dolomite, corrected for Cenozoic extensional tilting, has a declination of 16.9°, with an inclination of 29.5° ($k =$

1756.9, α95 = 1.8°; Table 1). The first ChRM held within the mineralized zebra rocks at Ely has a VGP that intersects the Middle Jurassic portion of the APWP. This ChRM is present is 3 of 4 ED sites. The second ChRM is only held within the ED4 sample site and contains a VGP that plots directly on the Middle Jurassic portion of the APWP. Unblocking temperatures of both ChRMs were between 480-580°C and were interpreted as being held in magnetite and/or titanomagnetite. The SEM and EDS analyses confirm the presence of small titanium enriched iron oxides in the ED3-7 that appeared to be precipitated authigenic magnetite in the interstitial pore spaces between dolomite rhombs. Both ChRMs held in the ED sample sites are interpreted to be CRMs.

The first CRM in the zebra dolomite at Ely is interpreted as younger than the host rock remagnetization that occurred during the Central Nevada Thrusting that persisted through the Middle Jurassic or possibly occurred during the initial stages of the Sevier Orogeny in the Late Jurassic. Hydrothermal fluids were expelled and then migrated through the Arcturus Formation that formed the zebra dolomites and carried the CRM at sample sites ED1-3.

The second CRM found only in zebra dolomites at sample site ED4, is interpreted as a slightly younger remagnetization than the first CRM that occurred during the initial stages of the Sevier Orogeny during the Late Jurassic. It is hypothesized that reactivation of previous fluid pathways from earlier deformation allowed for a secondary younger pulse of hydrothermal fluids to form the zebra dolomites and carried the CRM at sample site ED4 due to its close spatial relation to the other ED sample sites. The presence of hydrothermal alteration is also evident in thin section and SEM analysis. The habit of minerals coupled with EDS confirms that the titanium enriched iron oxides, likely carrying the CRMs, precipitated between dolomite rhombs and void spaces.

Eureka

Two ChRMs are observed in zebra dolomite specimens from the Cambrian Hamburg Formation at the Eureka sample site. The zebra dolomites were sampled. Determination of burial temperatures for the Hamburg Formation are believed to have ranged from 75-200°C related to significant hydrothermal activity near the Eureka Mining District, Nevada. These alterations have resulted in increased porosity of the Hamburg Formation (Diehl et al., 2010). Each ChRM component was plotted both geographically (without correction) and stratigraphically (with correction) due to uncertainties of the strike and dip of the EZD specimens at the sample locality. Mean directions were calculated for each of the two ChRM components of the Eureka zebra dolomites both geographically (without corrections) and stratigraphically (with Cenozoic corrections) as shown in Table 1.

The mean geographic direction of the first ChRM in the zebra dolomite has a declination of 324.4°, with an inclination of 54° (k = 24.72, α95 = 4°; Table 1). The mean geographic direction of the second ChRM in the zebra dolomite has a declination of 327.3°, with an inclination of 8.8° (k =21.84, α95 = 6.8°; Table 1).

The first geographic ChRM held within the mineralized zebra rocks at Eureka has a VGP that intersects the Middle Jurassic portion of the APWP and the second CRM from ED4. This ChRM is present at 6 of 9 EZD sites. The second ChRM is only present at EZD1 & EZD7 sample sites and contains a VGP that intersects the Middle to Late Triassic portion of the APWP. Unblocking temperatures of both ChRMs were between 360-580°C and were interpreted as being held in magnetite and/or titanomagnetite. The SEM and EDS analyses confirm the presence of large amounts of iron oxides in the EZD1-5 specimen that appeared to be precipitated authigenic magnetite forming in the interstitial pore spaces between dolomite rhombs and pores created by hydrothermal fluids. Both ChRMs (geographically and stratigraphically) held in the EZD sample sites are interpreted to be CRMs.

Mean stratigraphic directions were also calculated for each of the two ChRM components found at the Eureka sample locality. The mean stratigraphic direction of the first ChRM in the zebra dolomite, corrected for Cenozoic extensional tilting, has a declination of 44.9°, with an inclination of 23° (k = 24.72, α95 = 4°; Table 1). The mean stratigraphic direction of the second ChRM in the zebra dolomite, corrected for Cenozoic extensional tilting, has a declination of 355.3°, with an inclination of 23.7° (k =21.84, α95 = 6.8°; Table 1). Again, this second ChRM is only found at the EZD1 and EZD7 sample sites.

The first stratigraphic ChRM held within the mineralized zebra rocks at Eureka has a VGP that falls off of the APWP. This ChRM is present is 6 of 9 EZD sites. The second ChRM is only held within EZD1 & EZD7 sample sites and contains a VGP that intersects on the Late Triassic to Early Jurassic portion of the APWP. Again, both ChRMs are interpreted to be CRMs held in authigenic magnetite based on unblocking temperatures and petrography. Uncertainties in strike/dip and vertical axis rotation near the EZD sample sites are likely a factor in the discrepancies between the VGPs for both CRMs at EZD plotted geographically vs. stratigraphically. Both CRM components had significant Fisher statistics meaning there is high confidence in the mean directions. However, with uncertainty in the corrections, it is difficult to confidently and accurately interpret the age of the remagnetizations at the Eureka sample locality.

Northern Nevada

Wendover

Zebra dolomites sampled from Wendover are held within the Devonian Guilmette Formation. According to a U.S. Geological Survey report (1989), CAI values for the Guilmette Fm range from 3.5-5.5, corresponding to estimated maximum burial temperatures from 150-350°C. However, it is noted that at one collection the CAI was estimated to be as low as 3.0 (Karklins et al., 1989). The zebra dolomite samples at Wendover contain much more white saddle dolomite than previous locations. The Guilmette Formation host rock was heavily fractured and jointed with numerous white breccia masses at this location as described by Schneyer (1990).

At Wendover sample sites, stable ancient magnetizations were observed; however, they clustered near the Modern declination and inclination of Nevada (D=12°, I=63°). Further, errors during the sample collection process at Wendover do not permit calculations of VGPs for the few stable magnetizations present.

The magnetizations held in these samples are interpreted to reside in titanomagnetite based on unblocking temperatures of 460°C. Resampling of the Wendover zebra dolomites and their surrounding host rock could yield conclusive paleomagnetic data that would assist to date and explain the localized tectonics and fluid flow timing at this locality.

Summit

Zebra dolomites sampled from Summit are also held within the Devonian Guilmette Formation. Again, CAI values for the Guilmette Fm range from 3.5-5.5. This corresponds to estimated maximum burial temperatures from 150-350°C (Karklins et al., 1989). Also, the zebra dolomite samples at Summit contain much more white saddle dolomite than previous locations, similar to specimens collected from Wendover.

Although there is evidence of counterclockwise vertical axis rotation throughout the Basin and Range Province, no correction was used. Vertical axis rotation resulting from Cenozoic tectonics, range from 90° in the western portion of the state to no rotation in parts of eastern Nevada and are too far away from sampling locations to be interpolated to the Summit study area (Hudson et al., 1998) (Petronis et al., 2014) (Best et al., 2013) (McQuarrie & Wernicke, 2005).

A mean direction was calculated for the ChRM component of the Summit zebra dolomites. The mean stratigraphic direction of the ChRM in the zebra dolomite, corrected for Cenozoic extensional tilting, has a declination of 308.2°, with an inclination of 63.1° ($k = 57.15$, $\alpha_{95} = 12.3°$; Table 1). The ChRM held within the mineralized zebra rocks at Summit has a VGP that intersects the Late Jurassic portion of the APWP. The ChRM was only observed at SD1. The mineralogy of the magnetic carrier held in the Summit zebra dolomites is interpreted to be titanomagnetite based on unblocking between 400-480°C. This ChRM is interpreted to be a CRM.

The Summit zebra dolomites and the associated CRM are interpreted to be the product of hydrothermal fluid migration during the Sevier Orogeny in northern Nevada. The error ellipse for the Summit VGP is the largest observed in this study. This coupled with the relatively few samples collected from the locality, makes the authors hesitant to confidently interpret the exact age of the CRM, however, there is a remagnetization there with strong statistics. Future sampling and analysis of the Summit zebra dolomite locality would provide a more confident interpretation of the age of the zebra dolomites and their associated CRM at Summit.

The ChRMs held in these zebra dolomites at all sample site locations are interpreted at CRMs, acquired at relatively low temperatures due to tectonically driven fluids, although the mechanisms of acquisition of the magnetizations in each area are likely different. It is difficult to rule out a thermoviscous remanent magnetization (TVRM) for many of these samples. While geochemical analysis has given relative burial temperatures for the host rocks (or surrounding rocks), the time of burial at elevated temperatures is more difficult to determine. The active tectonics that occurred throughout Nevada's geologic history cannot rule out multiple exhumation events, which would make the acquisition of a TVRM less likely.

CONCLUSION

All magnetizations found within zebra dolomites in this study are interpreted as CRMs because of low burial temperatures of the host rock formations and evidence of hydrothermal flow seen in petrographic examination (i.e. fluid inclusion, saddle dolomite, porosity-filling iron oxides). The CRMs are held in magnetite, as evidenced by the unblocking temperatures, SEM analysis, and rock magnetic analysis. The unblocking temperatures within the zebra dolomite sites vary with varying Ti content. This variation further reinforces that the fluid flow events are likely different events, either in time or in fluid flow paths. Both EZD and ED are located close to each other in central Nevada, and the habits of the magnetic minerals and the different elemental concentrations seen in SEM support this conclusion.

The CRMs are associated with hydrothermal processes that are fairly low temperature, however these hydrothermal processes are all different. Some are associated with ore deposits; some are related to extensional and/or compressional tectonic activity. Probably all are exploiting faults in the area because the zebras here, and all around the world, are ubiquitously associated with faults. There is probably not one way zebra dolomites form, possibly on the molecular level, but they can form in a lot of different tectonic or hydrothermal systems. The complex tectonics of Nevada are reflected in the multiple formations of the zebra dolomites the multiple ages of magnetization acquisition within them.

We have found possible ages of different zebra dolomites at different locations in Nevada. Without extensive sampling of the host rocks at each location, we are unable to determine if the timing of magnetization within the zebra is exclusive to those zebra deposits and is therefore dating their formation, or if it is the same remagnetization seen within both host and zebra rocks. Previous studies of the zebra dolomites (Evans et al., 2012; Dulin, 2014) have shown that zebra dolomites and host rocks have similar directions. It is shown that the zebra dolomites provide conduits for fluid flow and have acquired remagnetizations that date these different fluid-flow events that have occurred during Nevada's complex history.

REFERENCES

Armstrong, R. L. (1968). Sevier Orogenic Belt in Nevada and Utah. *79*(4), 429–429. https://doi.org/10.1130/0016-7606(1968)79%5B429:sobina%5D2.0.co;2

Butler, R. F. (1992). Paleomagnetism: Magnetic Domains to Geologic Terranes: Tucson, AZ.

Beales, F. W., & Hardy, J. L. (1980). Criteria for the Recognition of Diverse Dolomite Types with an Emphasis on Studies of Host Rocks for Mississippi Valley-Type Ore Deposits. *SEPM (Society for Sedimentary Geology) EBooks*, 197–213. https://doi.org/10.2110/pec.80.28.0197

Best, M. G., Christiansen, E. H., Deino, A. L., Gromme, S., Hart, G. L., & Tingey, D. G. (2013). The 36–18 Ma Indian Peak–Caliente Ignimbrite Field and Calderas, Southeastern Great Basin, USA: Multicyclic Super-Eruptions. *Geosphere*, *9*(4), 864–950. https://doi.org/10.1130/ges00902.1

Blackford, N. R., Long, S. P., Stout, A., Rodgers, D. W., Cooper, C. M., Kramer, K., Di Fiori, R. V., & Soignard, E. (2021). Late Cretaceous Upper-Crustal Thermal Structure of the Sevier Hinterland: Implications for the geodynamics of the Nevadaplano. *Geosphere*. https://doi.org/10.1130/ges02386.1

Canada, A. S., Cassel, E. J., McGrew, A. J., Smith, M. E., Stockli, D. F., Foland, K. A., … Singer, B. S. (2019). Eocene exhumation and extensional basin formation in the Copper Mountains, Nevada, USA. Geosphere (Boulder, Colo.), 15(5), 1577–1597. https://doi.org/10.1130/GES02101.1

Carr, W. J., Geological Survey, & Geographical Surveys West of the 100th Meridian. (1988). *Geology of the Devils Hole area, Nevada by W.J. Carr.* Denver, Colo.: Dept. of the Interior, U.S. Geological

Survey : Books and Open-File Reports [distributor].

Centrella, S., Beaudoin, N. E., Koehn, D., Motte, G., Guilhem Hoareau, & Callot, J. P. (2022). How Fluid-Mediated Rock Transformations can Mimic Hydro-Fracturing Patterns in Hydrothermal Dolomite. *Marine and Petroleum Geology*, *140*, 105657–105657. https://doi.org/10.1016/j.marpetgeo.2022.105657

Dickinson, W. R. (2006). Geotectonic evolution of the Great Basin. *Geosphere*, *2*(7), 353. https://doi.org/10.1130/ges00054.1

Diehl, S. F., Hofstra, A. H., Koenig, A. E., Poul Emsbo, Christiansen, W. D., & Johnson, C. A. (2010). Hydrothermal Zebra Dolomite in the Great Basin, Nevada—Attributes and Relation to Paleozoic Stratigraphy, Tectonics, and Ore Deposits. *Geosphere*, *6*(5), 663–690. https://doi.org/10.1130/ges00530.1

Dulin, S. (2014). Paleomagnetism as a Tool for Determining Diagenetic, Depositional, and Erosional Events as Recorded in Sedimentary and Igneous Rocks. *University of Oklahoma.* Dissertation.

Ekren, E. B., Geological Survey , issuing body, U.S. Atomic Energy Commission, & United States. Army. Corps of Engineers. Manhattan District. (1971). *Geology of northern Nellis Air Force Base bombing and gunnery range, Nye County, Nevada / by E. B. Ekren [and three others]; prepared on behalf of the U.S. Atomic Energy Commission.*

Elmore, R. D., Bagley, D. S., London, D. (1991). Paleomagnetic Dating of Diagenesis by Basinal and Meteoric Fluids, Ordovician Carbonates, Arbuckle Mountains, Southern Oklahoma. *AAPG Bulletin*, *75*. https://doi.org/10.1306/20b240a6-170d-11d7-8645000102c1865d

Evans, S. C., Elmore, R. D., Dennie, D., & Dulin, S. A. (2012). Remagnetization of the Alamo Breccia, Nevada. *Geological Society London Special Publications*, *371*(1), 145–162. https://doi.org/10.1144/sp371.8

Ewing, A. (1930). Ferromagnetism and Hysteresis. *Proceedings (Physical Society (Great Britain) : 1926)*, *42*(5), 355–357. https://doi.org/10.1088/0959-5309/42/5/301

Fisher, R. (1953). Dispersion on a Sphere: Proceedings of the Royal Society of London. Series A, Mathematical and Physical Sciences, v. 217, no. 1130, p. 295-305.

Gillett, S. L., & Karlin, R. E. (2004). Pervasive late Paleozoic–Triassic Remagnetization of Miogeoclinal Carbonate Rocks in the Basin and Range and Vicinity, SW USA: Regional Results and Possible Tectonic Implications. *Physics of the Earth and Planetary Interiors*, *141*(2), 95–120. https://doi.org/10.1016/j.pepi.2003.11.001

Hudson, M. R., John, D. A., Conrad, J. E., & McKee, E. H. (2000). Style and Age of Late Oligocene-Early Miocene Deformation in the Southern Stillwater Range, West Central Nevada: Paleomagnetism, Geochronology, and Field Relations. *Journal of Geophysical Research*, *105*(B1), 929–954. https://doi.org/10.1029/1999jb900338

Kahya, A., Kuscu, E., & Yenice, F. İ. (2021). Genesis of the Zebra Dolomites and Relation to Carbonate-Hosted Au-Ag-Zn±Pb Deposits in the Maden Village (Ulukışla-Niğde), Central Taurides, South Turkey. *Bulletin of the Mineral Research and Exploration*, 1–13. https://doi.org/10.19111/bulletinofmre.877977

Kareem, K. H., Al-Aasm, I. S., & Mansurbeg, H. (2019). Structurally-Controlled Hydrothermal Fluid Flow in an Extensional Tectonic Regime: A Case Study of Cretaceous Qamchuqa Formation, Zagros Basin, Kurdistan Iraq. *Sedimentary Geology*, *386*, 52–78. https://doi.org/10.1016/j.sedgeo.2019.04.001

Karklins, O. L., Repetski, J. E., & Ketner, K. B. (1989). Maps Showing Ages and Thermal Maturation Values of Conodonts from the Goshute-Toano Range, Elko County, Nevada */ Department of the Interior, U.S. Geological Survey ; by Olgerts L. Karklins, John E. Repetski, and Keith B. Ketner.* Reston, Va.: The Survey ; a Denver, Colo. : For sale by Map Distribution.

Kelka, Beaudoin, N. E., Lorenz, J., Koehn, D., Klaus Regenauer-Lieb, Boyce, A., & Chung, P. (2023). Zebra Dolomites of the Spessart, Germany: Implications for Hydrothermal Systems of the European Zechstein Basin. *International Journal of Earth Sciences*, *112*(8), 2293–2311. https://doi.org/10.1007/s00531-023-02346-x

Kelka, U., Koehn, D., & Beaudoin, N. (2015). Zebra Pattern in Rocks as a Function of Grain Growth Affected by Second-Phase Particles. *Frontiers in Physics*, *3*. https://doi.org/10.3389/fphy.2015.00074

Kelka, U., Veveakis, M., Koehn, D., & Beaudoin, N. (2017). Zebra Rocks: Compaction Waves Create Ore Deposits. *Scientific Reports*, *7*(1). https://doi.org/10.1038/s41598-017-14541-3

Kent, D.V. (1985). Thermoviscous Remagnetization in some Appalachian Limestones. Geophysical Research Letters, 12, 805-808.

Lawton, T. F., Cashman, P. H., Trexler, J. H., & Taylor, W. J. (2017). The Late Paleozoic Southwestern Laurentian Borderland. *Geology*, G39071.1. https://doi.org/10.1130/g39071.1

Lesher, C. E., & Spera, F. J. (2015). Thermodynamic and Transport Properties of Silicate Melts and Magma. *The Encyclopedia of Volcanoes*, 113–141. https://doi.org/10.1016/b978-0-12-385938-

9.00005-5

Li, T., Zhu, D., Yang, M., Zhang, X., Li, P., Lu, C., & Zou, H. (2021). Early-Stage Marine Dolomite Altered by Hydrothermal Fluids in the Middle Permian Maokou Formation in the Eastern Sichuan Basin, Southern China. *Marine and Petroleum Geology*, *134*, 105367–105367. https://doi.org/10.1016/j.marpetgeo.2021.105367

Long, S. P., Henry, C. D., Muntean, J. L., Edmondo, G. P., & Cassel, E. J. (2014). Early Cretaceous Construction of a Structural Culmination, Eureka, Nevada, U.S.A.; Implications for Out-of-Sequence Deformation in the Sevier hinterland. *Geosphere (Boulder, Colo.)*, *10*(3), 564–584. https://doi.org/10.1130/GES00997.1

McCormick, C. A., Corlett, H., Clog, M., Boyce, A. J., Tartèse, R., Steele-MacInnis, M., & Hollis, C. (2023). Basin Scale Evolution of Zebra Textures in Fault-Controlled, Hydrothermal Dolomite Bodies: Insights from the Western Canadian Sedimentary Basin. *Basin Research*, *35*(5), 2010–2039. https://doi.org/10.1111/bre.12789

McQuarrie, N., & Wernicke, B. P. (2005). An Animated Tectonic Reconstruction of Southwestern North America since 36 Ma. *Geosphere (Boulder, Colo.)*, *1*(3), 147–172. https://doi.org/10.1130/GES00016.1

Morrow, D. W. (2014). Zebra and Boxwork Fabrics in Hydrothermal Dolomites of Northern Canada: Indicators for Dilational Fracturing, Dissolution or in situ Replacement? *Sedimentology*, *61*(4), 915–951. https://doi.org/10.1111/sed.12094

Middleton, M. F., and Schmidt, P. W. (1982). Paleothermometry of the Sydney Basin: Journal of Geophysical Research: Solid Earth, v. 87, no. B7, p. 5351-5359.

Petronis, M. S., Holm, D. K., Geissman, J. W., Hacker, D. B., & Arnold, B. J. (2014). Paleomagnetic Results from the Eastern Caliente-Enterprise Zone, Southwestern Utah: Implications for Initiation of a Major Miocene Transfer Zone. *Geosphere*, *10*(3), 534–563. https://doi.org/10.1130/ges00834.1

Pullaiah, G., Irving, E., Buchan, K. L., and Dunlop, D. J. (1975). Magnetization Changes Caused by Burial and Uplift.: Earth and Planetary Science Letters, v. 28, p. 133-143.

Schneyer, J. D. (1990). Geologic Map of the Leppy Peak Quadrangle and Adjacent Area, Elko County, Nevada, and Tooele County, Utah */ Department of the Interior, U.S. Geological Survey ; by Joel D. Schneyer.* Reston, Va. : Denver, Colo.: The Survey ; For sale by Map Distribution. Print.

Shenton, B. J., Grossman, E. L., Passey, B. H., Henkes, G. A., Becker, T. P., Laya, J. C., Perez-Huerta, A., Becker, S. P., & Lawson, M. (2015). Clumped Isotope Thermometry in Deeply Buried Sedimentary Carbonates: The Effects of Bond Reordering and Recrystallization. *Geological Society of America Bulletin*, B31169.1. https://doi.org/10.1130/b31169.1

Speed, R. C., & Sleep, N. H. (1982). Antler Orogeny and Foreland Basin: A Model. *Geological Society of America Bulletin*, *93*(9), 815. https://doi.org/10.1130/0016-7606(1982)93%3C815:aoafba%3E2.0.co;2

Stewart, J. H. (1980). Regional Tilt Patterns of Late Cenozoic Basin-Range Fault Blocks, Western United States. *Geological Society of America Bulletin*, *91*(8), 460. https://doi.org/10.1130/0016-7606(1980)91%3C460:rtpolc%3E2.0.co;2

Torsvik, T. H., Voo, R. V. d., Preeden, U., Niocaill, C. M., Steinberger, B., Doubrovine, P. V., Hinsbergen, D. J. J. v., Domeier, M., Gaina, C., Tohver, E., Meert, J. G., McCausland, P. J. A., and Cocks, L. R. M. (2012). Phanerozoic Polar Wander, Palaeogeography and Dynamics: *Earth-Science Reviews*, v. 114, p. 325-368.

Vandeginste, V., John, C. M., Cosgrove, J. W., & Manning, C. (2014). Dimensions, Texture-Distribution, and Geochemical Heterogeneities of Fracture–Related Dolomite Geobodies Hosted in Ediacaran Limestones, Northern Oman. *AAPG Bulletin*, *98*(9), 1789–1809. https://doi.org/10.1306/05121413127

Vandeginste, Swennen, R., Gleeson, S. A., Ellam, R. M., Osadetz, K., & Francois, R. (2005). Zebra Dolomitization as a Result of Focused Fluid Flow in the Rocky Mountains Fold and Thrust Belt, Canada. *Sedimentology*, *52*(5), 1067–1095. https://doi.org/10.1111/j.1365-3091.2005.00724.x

Vandeginste, Swennen, R., Gleeson, S. A., Ellam, R. M., Osadetz, K., & François Roure. (2007). Geochemical Constraints on the Origin of the Kicking Horse and Monarch Mississippi Valley-Type Lead-Zinc Ore Deposits, Southeast British Columbia, Canada. *Mineralium Deposita*, *42*(8), 913–935. https://doi.org/10.1007/s00126-007-0142-6

Xu, Zhou, G., Wan, C., Zhang, L., Tao, J., Xu, C., & Yan, X. (2022). Geochemical Characteristics and Fluid Properties of the Qixia Formation Dolomites of the Middle Permian in the Shuangyushi Block, NW Sichuan Basin, China. *Frontiers in Earth Science*, *10*. https://doi.org/10.3389/feart.2022.904932

Zijderveld, J. D. A. (1967). A.C. Demagnetization of Rocks: Analysis of Results, *in* Collison, D. E., K.M.Creer, and Runcorn, S. K., eds., *Methods in Paleomagnetism: New York*, El Sevier Science, p. 254-286.